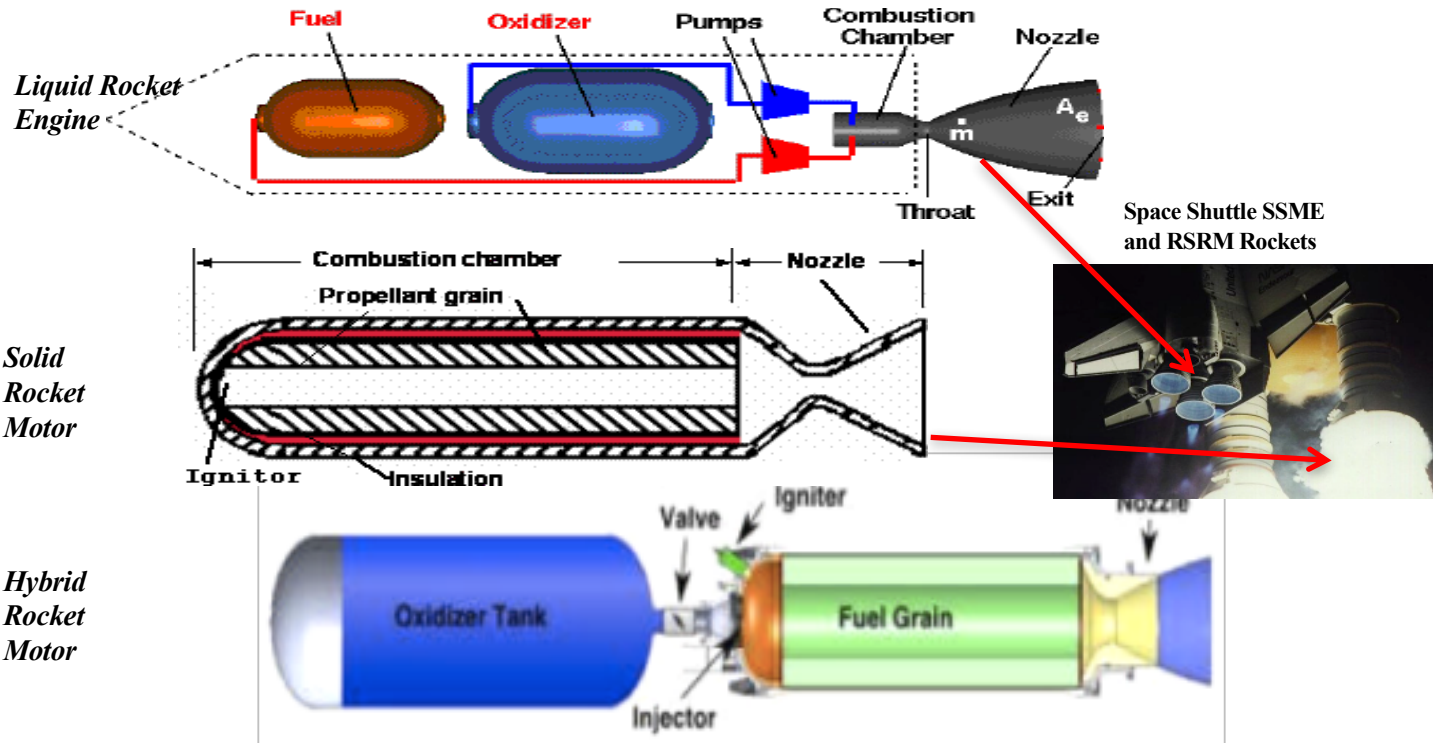


Lecture 3.1: Introduction to Hybrid Rockets

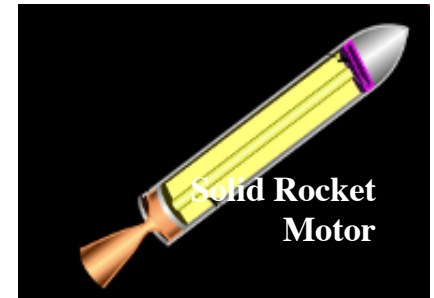


- Sutton and Biblarz: Chapter 15, Appendix 4 ...

Chemical Rockets

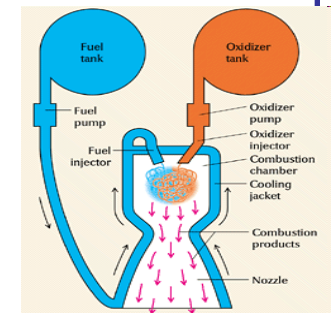
Solid Rockets

Oxidizer and fuel are chemically mixed together at the molecular level to form a solid fuel grain. Once ignited, they cannot be stopped, throttled, or restarted.



Liquid Rockets

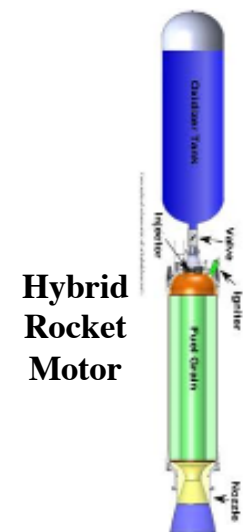
In a bi-propellant liquid rocket, an oxidizer and fuel are mixed in the combustion chamber. Oxidizer is usually maintained at cryogenic temperatures, typically requiring turbo pumps. Mono-propellant liquid rockets use a material which combusts in the presence of a catalyst. Liquid rockets can be throttled, stopped, and restarted.



Liquid Rocket Engine

Hybrid Rockets

Possess features of both liquid and solid rockets. A hybrid consists of a solid fuel grain made from a polymeric material. The oxidizer is stored in a tank separate from the fuel grain, which is stored in a combustion chamber. Both propellants are inert and only combust when the fuel is converted to gaseous state and mixed with oxidizer in the combustion chamber. Like liquid rockets, hybrid rockets can be throttle, stopped, and restarted.



Hybrid Rocket Motor

Chemical Rocket Comparison

Feature	Liquid, Bipropellant	Solid	Hybrid
Safety	Potential for combustion instability, can explode, volatile propellants	Highly flammable significant explosion potential, DOT 1.1	Inert propellants, low explosion and transport risk
Toxicity	Ranges from non-toxic to highly toxic	Exhaust products highly toxic	Exhaust products non-toxic (CO₂, H₂O)
Fabrication Costs	Extremely expensive	Expensive, mostly due to handling difficulties	Inexpensive
Complexity/Reliability	Highly complex, moderate reliability	Simple-to-moderate complexity, high reliability	Moderate complexity, high reliability
Operation	Throttleable, restartable, high performance	No restart, throttle capability, high-to-moderate performance	Potentially, Throttleable, restartable, moderate performance

Space Dev® Hybrid Powered “Spaceship 1”

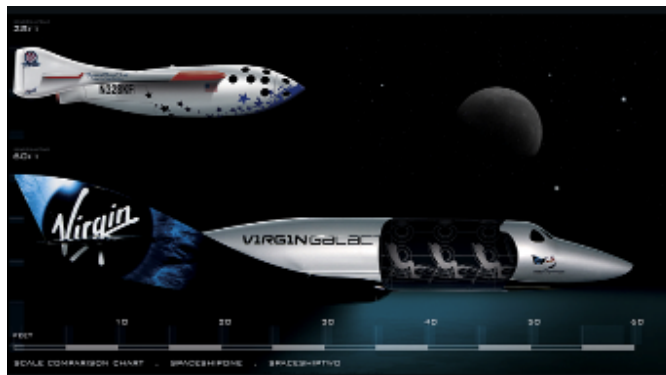


- Built by Burt Rutan (Scaled Composites®) with Paul Allen’s (Apple co founder) Money in Mojave CA SS1 wrote history, when the first private suborbital spaceflight was conducted on June 21, 2004 (with pilot Mike Melvill).
- SS1 won the [X-Prize](#) with flights on 29.09.2004 (Melville) and a follow up flight on 04.10.2004. (Brian Binneie)
- Powered by a 16700 lbf thrust Hybrid Motor (SpaceDev)



Virgin Galactic, the British company created by entrepreneur Sir Richard Branson to send tourists into space and the State of New Mexico have entered into an agreement for the State to build a \$225 million spaceport. Virgin Galactic has also revealed that 38,000 people from 126 countries have expressed interest its commercial suborbital flights. A core group of 100 "founders" have paid the full initial \$200,000 ticket price and an additional 300 intrepid passengers have placed deposits.

Virgin Galactic was cleared for civil airspace operations in 2008 and is expected to initiate passenger services beginning in 2012.



Hybrids Rockets are a Potentially Enabling Technology for the Emerging Commercial Spaceflight Industry

- NASA is contracting with commercial space hardware and launch service companies to fill the void left by the retirement of the Space Shuttle fleet.
- Well funded firms like Virgin Galactic, SpaceX, Blue Origin, Sierra Nevada Corp, Bigelow Aerospace, and others are pioneering a new era in spaceflight and space exploration.



*Space X Falcon
9 Medium Lift
Launcher*



*SNC Dream Chaser
Powered by SNC Hybrid
Rocket Motor*



*Masten Engineering's
Winning Lunar X-
prize Entry*



*Danish Suborbital's Tycho
Brahe Spacecraft powered by
Hybrid HEAT Rocket*



*Bigelow Aerospace
Space Station Module*



*Spaceship One™ Hybrid
Rocket Firing During
Ansari X-prize Flight*

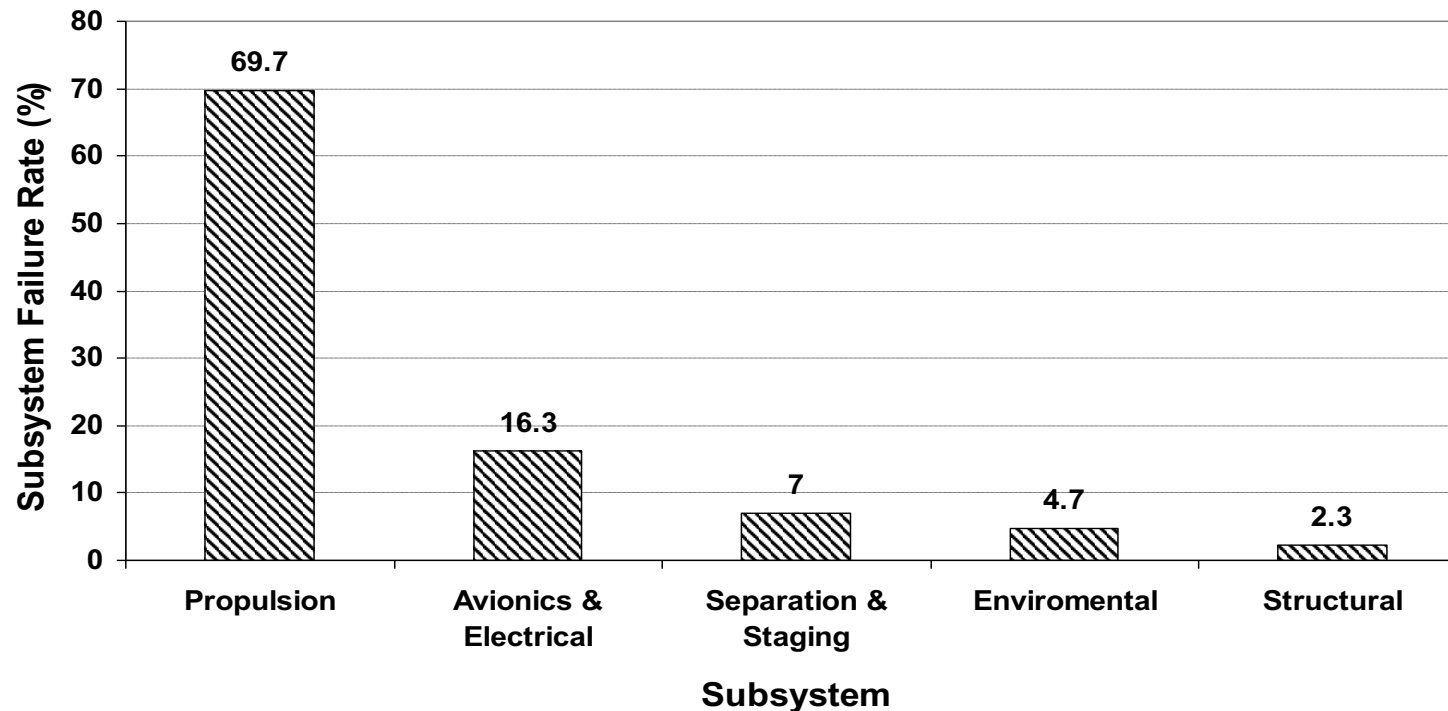


*Virgin Galactic VSS
Enterprise Powered by SNC
Hybrid Rocket Motor*

Launch System Safety

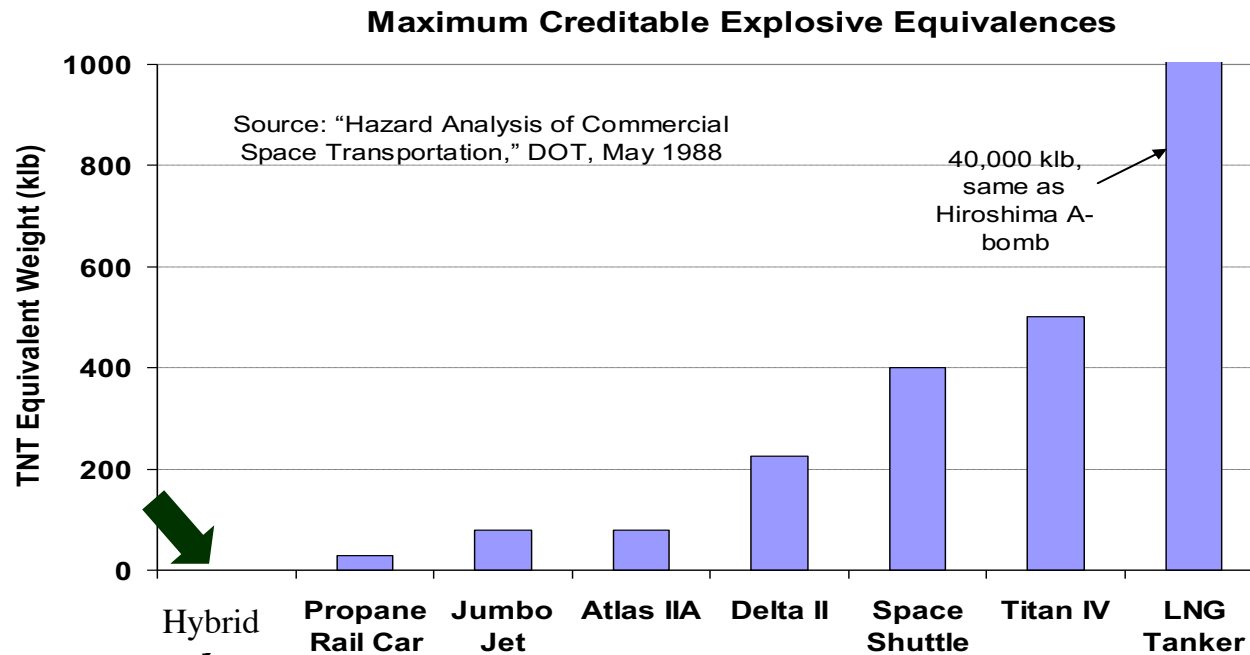
Almost 70% of all space launch failures are attributable to either the solid or liquid rocket propulsion system, either as a result of their complexity (liquids) or their explosive nature (solids and liquids).

Catastrophic Space Launch Vehicle Failures
(Data for 1,176 launches)



Rocket Safety (2)

The below chart puts the potential explosive force of both liquid and solid rockets in perspective, and explains why their use for commercial space transport and many other applications are not recommended.



Hybrid Rocket Motors

- Limited explosion potential, safer than liquid and pre-mixed solids
- Potential for restart and throttling
- Good Volumetric Efficiency, Bulk Density better than Liquid
not quite as compact as solid motor
- Exhaust Products typically benign, unlike solid exhaust plumes
- Insensitive to cracks or aging of fuel grain ... almost
infinite storability of fuel grain
- Low regressions rates compared to Solids ... allows for
“controlled” impulse, but requires bigger port area for
a given thrust
- Mixture ratio strongly influenced by port design ... fuel burn is
generally incomplete ... lower effective mass fraction

Hybrid Rocket Motors (cont'd)

• Fuels

- Hydroxy-terminated polybutadiene $(C_4H_6)_n(OH)_2$
- Acrylonitrile-Butadiene-Styrene (ABS)
- Plexiglass --polymethly-methacrylate -- PMMA $(C_5H_8O_2)$
- Burning enhancements include carbon or aluminum powder added to grain

• Oxidizers

- LOX (O_2)
 - ... Higher I_{sp} , dangerous to handle
 - ... Limited Storability
- Nitrous Oxide (N_2O)
 - ... Lower I_{sp} , safe for handling
 - ... highly storable
- Hydrogen Peroxide (H_2O_2)
 - ... Highest effective I_{sp} , very toxic
 - ... Highly storable

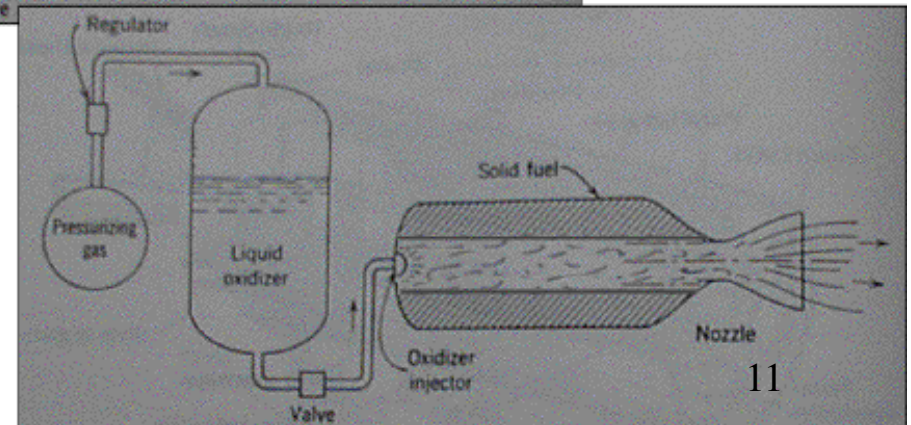
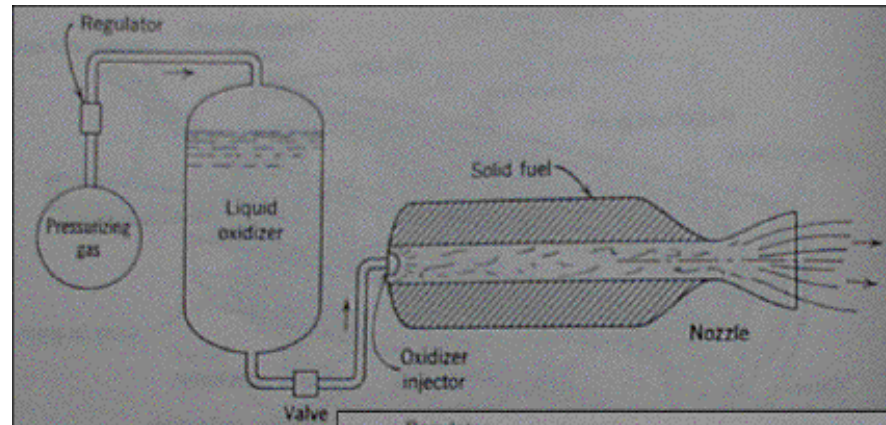
Transient Operation Model For Hybrid Rockets

- Revisit General Model

$$\frac{\partial P_0}{\partial t} + P_0 \left[\frac{1}{V_c} \frac{\partial V_c}{\partial t} + \frac{A^*}{V_c} \sqrt{\gamma R_g T \left(\frac{2}{\gamma + 1} \right)^{\frac{\gamma + 1}{\gamma - 1}}} \right] = \frac{R_g T_0}{V_c} \left[\dot{m}_{propellant} \right]$$

- For Hybrid Rocket Motors

$$\frac{\partial V_c}{\partial t} \neq 0$$



Transient Operation of Hybrid Rockets (cont'd)

- Following earlier analysis procedure used for solid motors

$$\frac{\partial P_0}{\partial t} + P_0 \left[\frac{1}{V_c} \frac{\partial V_c}{\partial t} + \frac{A^*}{V_c} \sqrt{\gamma R_g T \left(\frac{2}{\gamma + 1} \right)^{\frac{\gamma+1}{\gamma-1}}} \right] = \frac{R_g T_0}{V_c} \left[\dot{m}_{propellant} \right]$$

$$\frac{\partial V_c}{\partial t} = A_{burn} \dot{r}_{fuel} \rightarrow \left[\begin{array}{l} A_{burn} = \text{Grain Surface Burn Area} \\ r = \text{Grain Linear Regression Rate} \end{array} \right]$$

$$\dot{m}_{propellant} = \dot{m}_{ox} + \rho_{fuel} A_{burn} \dot{r}_{fuel}$$

Hybrid Rockets (cont'd)

- Substituting in for propellant mass flow

$$\frac{\partial P_0}{\partial t} + P_0 \left[\frac{A_{burn} \dot{r}_{fuel}}{V_c} + \frac{A^*}{V_c} \sqrt{\gamma R_g T \left(\frac{2}{\gamma + 1} \right)^{\frac{\gamma+1}{\gamma-1}}} \right] = \frac{R_g T_0}{V_c} \left[\dot{m}_{ox} + \rho_{fuel} A_{burn} \dot{r}_{fuel} \right]$$

→ Rearranging

$$\frac{\partial P_0}{\partial t} = \frac{R_g T_0}{V_c} \dot{m}_{ox} + \frac{R_g T_0}{V_c} \left[\rho_{fuel} A_{burn} \dot{r}_{fuel} \right] - P_0 \frac{A_{burn} \dot{r}_{fuel}}{V_c} - P_0 \left[\frac{A^*}{V_c} \sqrt{\gamma R_g T \left(\frac{2}{\gamma + 1} \right)^{\frac{\gamma+1}{\gamma-1}}} \right]$$

→ Collecting terms

Injector Massflow

$$\frac{\partial P_0}{\partial t} = \frac{R_g T_0}{V_c} \dot{m}_{ox} + \frac{A_{burn} \dot{r}_{fuel}}{V_c} \left[\rho_{fuel} R_g T_0 - P_0 \right] - P_0 \left[\frac{A^*}{V_c} \sqrt{\gamma R_g T \left(\frac{2}{\gamma + 1} \right)^{\frac{\gamma+1}{\gamma-1}}} \right]$$

Injector Design

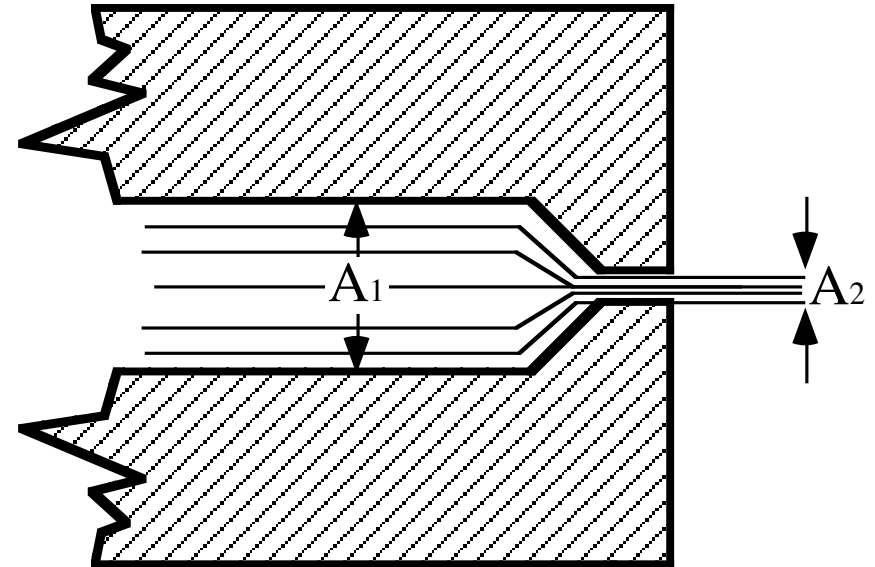
$$V_{2_{actual}} \equiv C_d \sqrt{2 \left(\frac{P_1 - P_2}{\rho} \right)}$$

- Define Volumetric Flow as

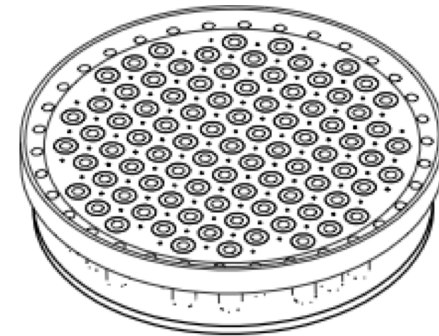
$$Q_v = A_2 V_{2_{actual}} = A_2 C_d \sqrt{2 \left(\frac{P_1 - P_2}{\rho} \right)}$$

- Finally Massflow is

$$\dot{m} = \rho Q_v = A_2 C_d \sqrt{2 \rho (P_1 - P_2)}$$



- ***Incompressible Discharge Coefficient Formula***



Hybrid Rocket Chamber Pressure Equation

- Following earlier analysis procedure for Oxidizer mass flow

$$\dot{m}_{ox} = A_{ox} C_{d_{ox}} \sqrt{2\rho_{ox} (p_{ox} - P_0)}$$

• *Incompressible Discharge Coefficient Formula*

$$\frac{\partial P_0}{\partial t} = \frac{A_{burn} \dot{r}_{fuel}}{V_c} \left[\rho_{fuel} R_g T_0 - P_0 \right] - P_0 \left[\frac{A^*}{V_c} \sqrt{\gamma R_g T_0 \left(\frac{2}{\gamma + 1} \right)^{\frac{\gamma+1}{\gamma-1}}} \right] + \frac{R_g T_0}{V_c} A_{ox} C_{d_{ox}} \sqrt{2\rho_{ox} (p_{ox} - P_0)}$$

Model for hybrid combustion pressure.

Term Due to Choking Mass
Flow Through Nozzle

$$\frac{\partial p_0}{\partial t} = \frac{A_{\text{burn}} \dot{r}}{V_c} \left[\rho_{\text{fuel}} R_g T_0 - p_0 \right] - p_0 \left[\frac{A^*}{V_c} \sqrt{\gamma R_g T_0 \left(\frac{2}{\gamma + 1} \right)^{\frac{\gamma+1}{\gamma-1}}} \right] + \frac{R_g T_0}{V_c} A_{\text{ox}} C_{d_{\text{ox}}} \sqrt{2 \rho_{\text{ox}} (p_{\text{ox}} - p_0)}$$

Fuel Vaporization Term

Oxidizer Entering Combustion
Chamber

- Also need relation for combustion pressure for complete motor simulation
- Derived from simple mass balance

Fuel Grain Regression Model for Hybrid Rockets

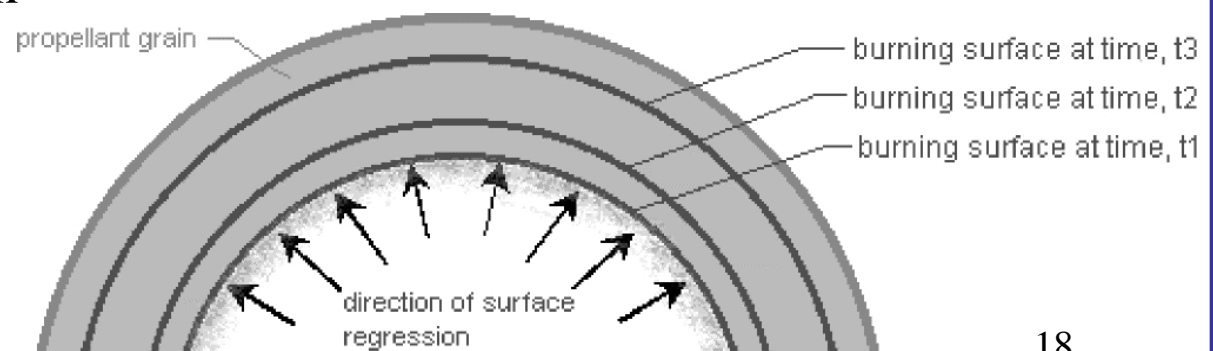
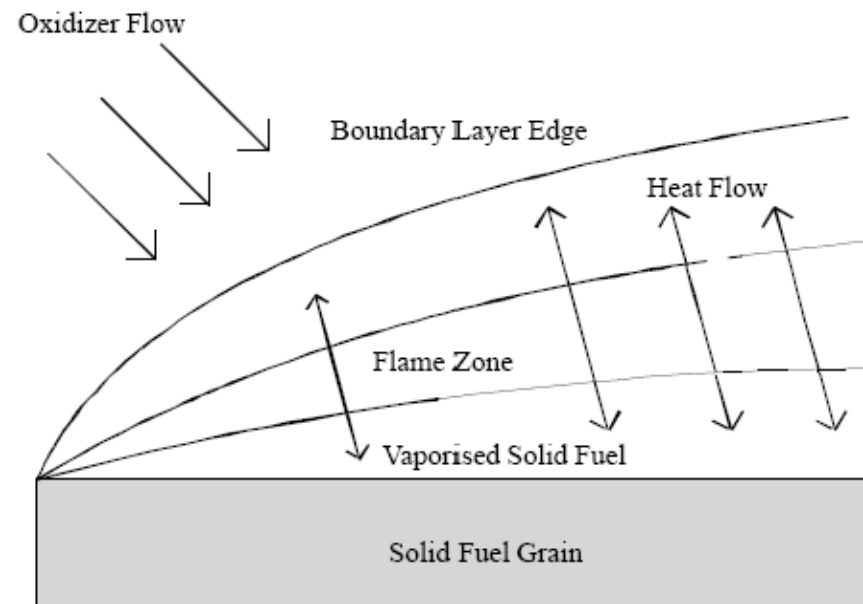
$$\frac{\partial P_0}{\partial t} = \frac{A_{burn} \dot{r}_{fuel}}{V_c} [\rho_{fuel} R_g T_0 - P_0] - P_0 \left[\frac{A^*}{V_c} \sqrt{\gamma R_g T_0 \left(\frac{2}{\gamma + 1} \right)^{\frac{\gamma+1}{\gamma-1}}} \right] + \frac{R_g T_0}{V_c} A_{ox} C_{d_{ox}} \sqrt{2 \rho_{ox} (p_{ox} - P_0)}$$

- Need *accurate expression for regression rate*, Saint Robert's Law is inaccurate and basically “incorrect” physical representation for Hybrid Rockets
- Very Limited Pressure Coupling with Hybrid regression rate

$$\dot{r} \neq a p^n$$

Enthalpy Balance Regression Model History

- Marxman and Gilbert outlined the basics of hybrid combustion in 1963
- Assumptions
 - Regression dominated by diffusion and not chemical kinetics
 - Flow is turbulent over entire fuel grain (early transition due to mass addition)
- Additional research has been completed for modes where radiation or kinetics dominate, but the diffusion relations remain mostly unaltered since their conception



The Classic Marxman and Gilbert Relation

Total Mass Flux (Oxidizer + Fuel)

$$\dot{r} = \frac{.036}{\rho_f} \left(\frac{\mu_\infty}{x} \right)^{0.2} \frac{G_{bx}^{0.8} B^{.23}}{\text{Pr}^{0.7}}$$

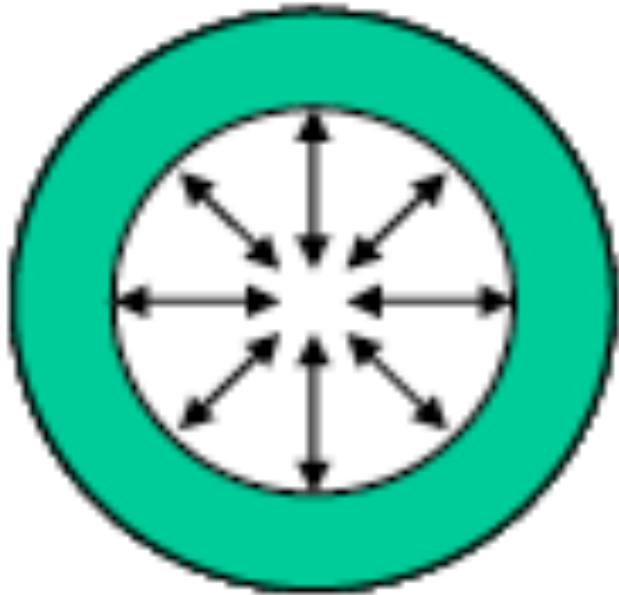
Blowing Coefficient

- Prandtl Number ... was assumed to be unity in initial Application of model
- Prandtl Number Definitely NOT Unity in practice

The Classic Marxman and Gilbert Relation

Total Mass Flux (Oxidizer + Fuel)

- Blowing Coefficient .. accounts for radial out gassing from fuel pyrolysis ... pushes flame zone away from fuel surface ... reduces convective heat transfer, surface skin friction



$$\beta \approx \frac{\Delta h_{flame}}{h_v}$$

Lee's Correlation

$$\frac{C_{f_{blow}}}{C_{f_0}} = \frac{1.27}{\beta^{0.77}}$$

Sutton, G. P., and Biblarz, O.,
Rocket Propulsion Elements,
John Wiley and Sons, New
York, 2001, Appendix 4, 5, pp.
731-737.

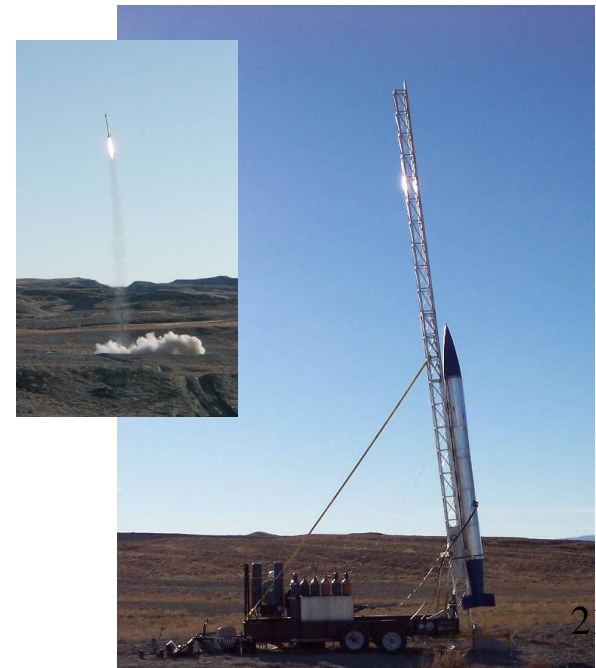
Classical Model Problems

- Empirical observations have shown that depending on the propellants used, regression exponent n not exactly as predicted by the Marxman model
- Instead n tends to range between 0.3 to 0.8. Values less than $n = 0.3$ or greater than $n = 0.8$ are not typically observed.
- Simplified empirical relation is often used instead of complete formulation
- Empirical Correlations
 - Do not scale well
 - Based upon configuration specific empirical data

$$\dot{r} = \frac{.036}{\rho_f} \left(\frac{\mu_\infty}{x} \right)^{0.2} \frac{G^{0.8} B^{.23}}{\text{Pr}^{0.7}}$$

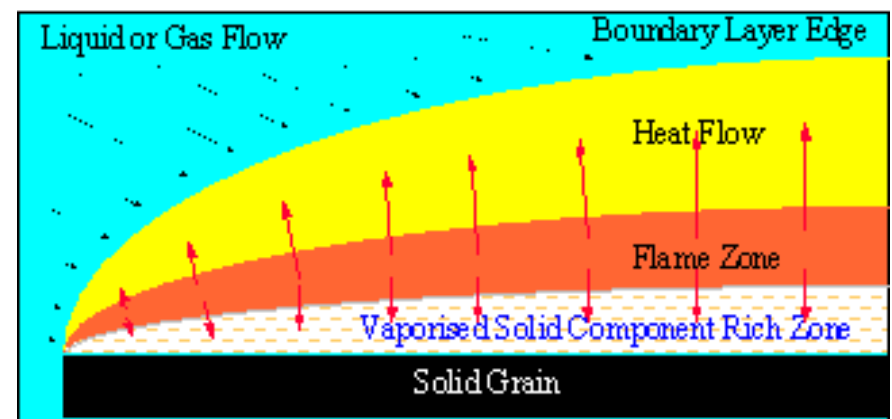
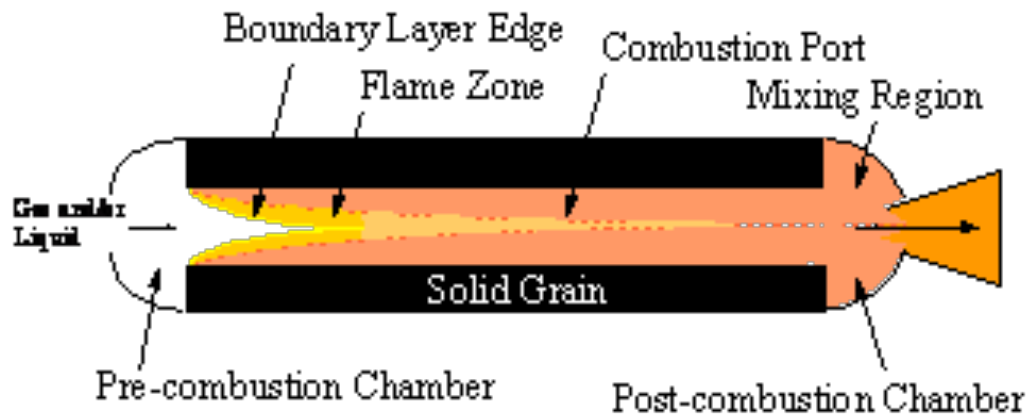
↓

$$\dot{r} = aG^n ? \text{ or } \dot{r} = a \frac{G^n}{x^{0.2}} ?$$

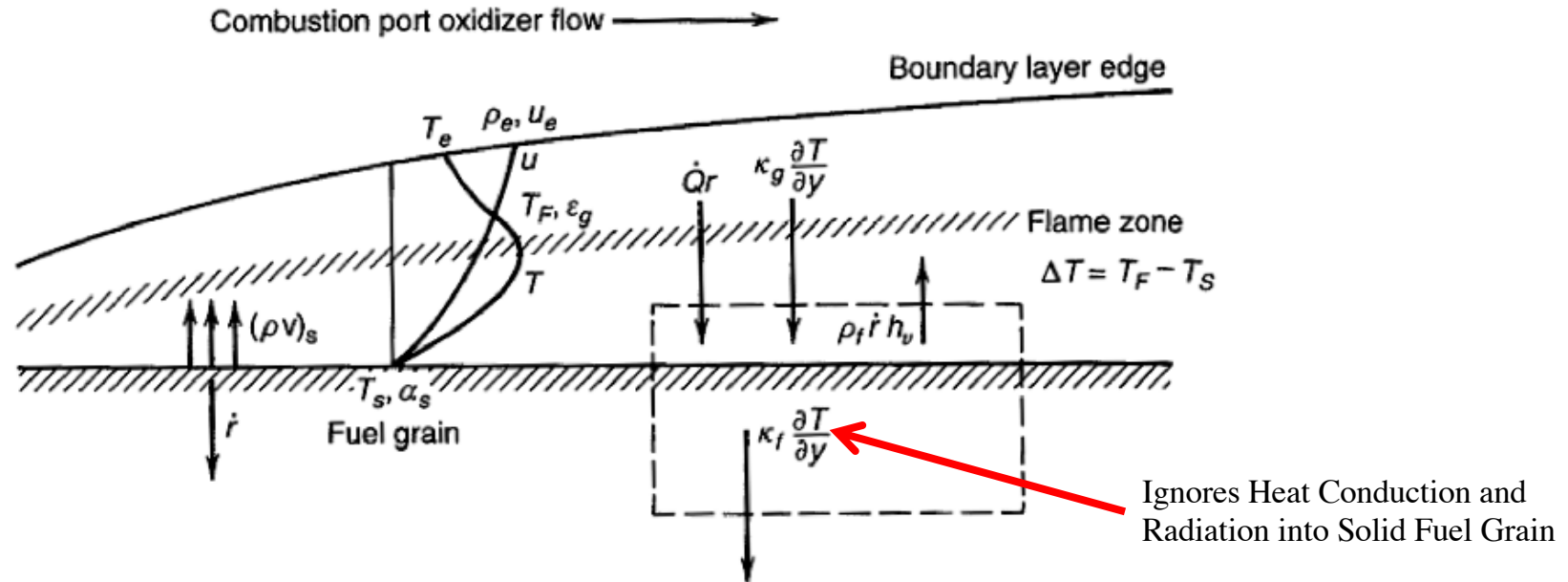


Enthalpy-Balance Fuel Grain Regression Model for Hybrid Rockets

- In hybrids separation of oxidizer and fuel into two different states leads to combustion different from that of either solid or liquid rockets.
- Combustion occurs as a macroscopic diffusion flame in which oxidizer-to-fuel ratio varies down length of solid grain.
- Hot gases cause vaporization of a small layer of solid.
- Vaporized solid reacts with rest of injected Ox component.
- Eventually, self-sustained combustion occurs.



Enthalpy Balance Regression Model Derivation



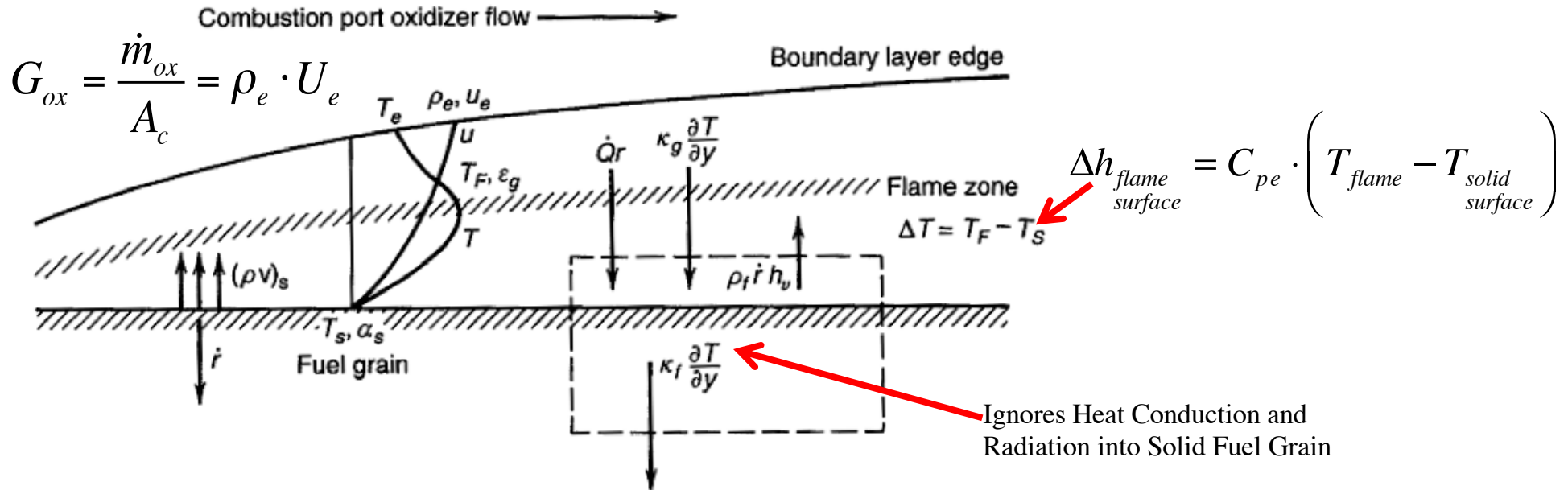
• *Heat transferred from flame to wall = energy of ablation*

$$\dot{q}_{convection} = \dot{q}_{fuel \text{ phase change}} = \rho_{fuel} \dot{r} h_v \rightarrow \{ h_v \equiv \text{latent heat of vaporization of fuel, } J / kg \}$$

• “Stanton number” ... proportional to
{ (heat transferred) / (thermal capacity of fluid) }

$$\rho_{fuel} \dot{r} h_v = H [T_{flame} - T_{surface}] = S_t \rho_e U_e C_{p_e} [T_{flame} - T_{surface}]$$

Enthalpy Balance Regression Model Derivation



- **Heat transferred from flame to wall = energy of ablation**

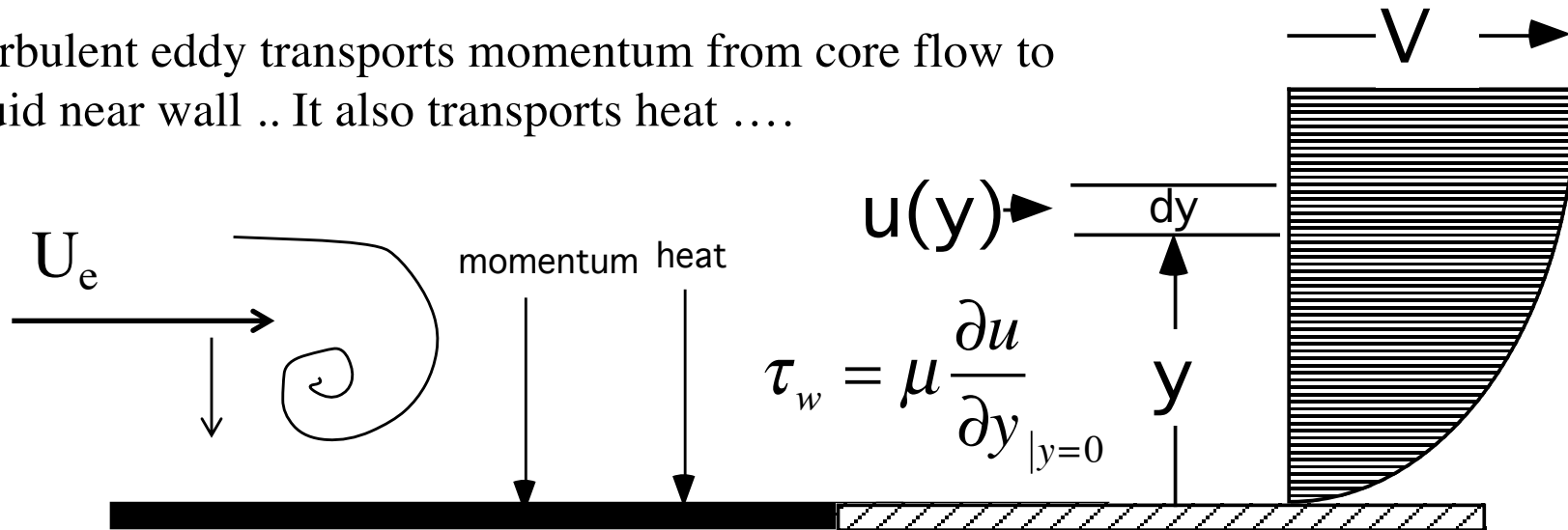
$$\dot{q}_{convection} = \dot{q}_{fuel\ phase\ change} = \rho_{fuel} \dot{r} h_v \rightarrow \left\{ h_v \equiv \text{latent heat of vaporization of fuel, } J / kg \right\}$$

• “Stanton number” ... proportional to
 $\left\{ \frac{\text{heat transferred}}{\text{thermal capacity of fluid}} \right\}$

$$\rho_{fuel} \dot{r} h_v = S_t \rho_e U_e C_{pe} [T_{flame} - T_{surface}] = S_t \rho_e U_e \Delta h_{flame\ surface}$$

Enthalpy Balance Regression Model Derivation (2)

- Reynold's Analogy ... correlation of heat transfer to skin friction
- Turbulent eddy transports momentum from core flow to fluid near wall .. It also transports heat



- Hard to Prove ... easy to use



$$0.5 \leq P_r \leq 1.0 \text{ for } \textit{turbulent flow}$$

$$S_t = \frac{C_f}{2} P_r^{-2/3} \rightarrow$$

C_f = skin friction coefficient, Pr = Prandtl Number

Enthalpy Balance Regression Model Derivation (3)

- Modified Reynolds Analogy Used to Relate Turbulent Heat Transfer to Surface Skin Friction (*Non-unity Prandtl Number*)

$$\rho_{\text{fuel}} \dot{r} h_v = H [T_{\text{flame}} - T_{\text{surface}}] = S_t \rho_e U_e C_{p_e} [T_{\text{flame}} - T_{\text{surface}}]$$

Reynold's Analogy

$$S_t = \frac{C_f}{2} \text{Pr}^{-2/3} \rightarrow$$

C_f = skin friction coefficient, Pr = Prandtl Number

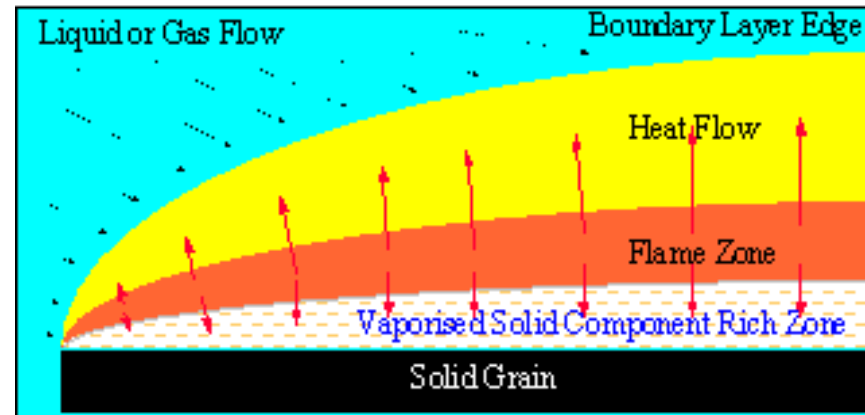
• Reynold's Analogy ... correlation of heat transfer to skin friction

- **Solve for regression rate**

$$\dot{r} = \left(\frac{C_f}{2} P_r^{-\frac{2}{3}} \right) \left(\frac{\rho_e \cdot U_e}{\rho_{\text{fuel}}} \right) \left(\frac{\Delta h_{\text{flame}}}{h_f} \right) \left(\frac{c_p [T_0 - T_{\text{fuel}}]}{h_v} \right) = \left(\frac{C_f}{2} P_r^{-\frac{2}{3}} \right) \left(\frac{\rho_e \cdot U_e}{\rho_{\text{fuel}}} \right) \left(\frac{\Delta h_{\text{flame}}}{h_f} \right)$$

Wall Blowing Correction

- Blowing Coefficient .. accounts for radial out gassing from fuel pyrolysis ... pushes flame zone away from fuel surface ... reduces convective heat transfer, surface skin friction



$\beta =$ "Blowing Coefficient"

$$\beta \equiv \frac{\text{Wall Shearing Force Due to Radial Outflow}}{\text{Wall Shearing Force Due to Skin Friction}} = \frac{\dot{m}_{\text{fuel}} \cdot U_e}{\tau_{\text{wall}} \cdot A_{\text{wall}}}$$

27

Wall Blowing Correction (2)

$$\beta \equiv \frac{\text{Wall Shearing Force Due to Radial Outflow}}{\text{Wall Shearing Force Due to Skin Friction}} = \frac{\dot{m}_{fuel} \cdot U_e}{\tau_{wall} \cdot A_{wall}}$$

$$\begin{aligned} \rightarrow \quad & V_{r_{wall}} = \dot{r} \\ & \dot{m}_f = \rho_{fuel} \cdot A_{wall} \cdot \dot{r} \\ & \tau_{wall} \cdot A_{wall} = \left(\frac{1}{2} \cdot \rho_e \cdot U_e^2 \right) \cdot C_f \cdot A_{wall} \end{aligned} \quad \rightarrow \beta = \frac{\rho_{fuel} \cdot A_{wall} \cdot \dot{r} \cdot U_e}{\left(\frac{1}{2} \cdot \rho_e \cdot U_e^2 \right) \cdot C_f \cdot A_{wall}}$$

$$\text{Simplifying} \rightarrow \beta = \left(\frac{\rho_{fuel} \cdot \dot{r}}{\rho_e \cdot U_e} \right) \cdot \frac{1}{C_f / 2}$$

Wall Blowing Correction (3)

$$\beta = \left(\frac{\rho_{fuel} \cdot \dot{r}}{\rho_e \cdot U_e} \right) \cdot \frac{1}{C_f / 2}$$

$$\text{Reynold's Analogy} \rightarrow C_f / 2 = S_t \cdot P_r^{2/3} \rightarrow \beta = \left(\frac{\rho_{fuel} \cdot \dot{r}}{\rho_e \cdot U_e \cdot S_t \cdot P_r^{2/3}} \right)$$

$$\text{But from Earlier} \rightarrow \rho_e \cdot U_e \cdot S_t = \frac{\rho_f \cdot \dot{r} \cdot h_v}{c_p [T_0 - T_{fuel}]} \rightarrow \frac{\rho_f \cdot \dot{r}}{\rho_e \cdot U_e \cdot S_t} = \frac{h_v}{c_p [T_0 - T_{fuel}]}$$

$$\text{Solving for} \rightarrow \beta = \frac{\rho_{fuel} \cdot \dot{r}}{\rho_e \cdot U_e \cdot S_t} \frac{1}{P_r^{2/3}} = \frac{h_v}{c_p [T_0 - T_{fuel}]} \frac{1}{P_r^{2/3}} = \frac{h_v}{\Delta h_{flame}} \cdot \frac{1}{P_r^{2/3}}$$

Wall Blowing Correction (4)

--> Correction for surface blowing

- Lee's Empirical Correlation -- Appendix 4, Sutton and Biblarz.
- Blowing Reduces the surface skin friction compared to “normal” boundary layer skin friction

$$\beta = \frac{h_v}{\Delta h_{flame}} \cdot \frac{1}{P_r^{2/3}}$$

$$\frac{C_{f_{blowing}}}{C_{f_0}} = \frac{1.27}{\beta^{0.77}} \cdot \sqrt{P_r} = \frac{1.27}{\left(\frac{h_v}{\Delta h_{flame}}\right)^{0.77}} \cdot P_r^{\frac{1}{2} - \left(\frac{2}{3}\right) \cdot 0.77} = 1.27 \left(\frac{h_v}{\Delta h_{flame}}\right)^{-0.77} \cdot P_r^{-0.0133}$$

$$0.5 \leq P_r \leq 1.0 \text{ for turbulent flow} \rightarrow 1 \leq P_r^{-0.0133} \leq 1.00929 \approx 1$$

Wall Blowing Correction ⁽⁵⁾

Allowing blowing-corrected skin friction to substitute for local skin friction coefficient "blowing adjusted" regression rate model

$$\frac{C_{f_{blowing}}}{C_{f_0}} = \frac{1.27}{\beta^{0.77}} \cdot \sqrt{P_r} \approx 1.27 \left(\frac{h_v}{\Delta h_{flame}} \right)^{-0.77}$$

$$\dot{r} = \left(\frac{\rho_e \cdot U_e}{P_r^{2/3} \cdot \rho_{fuel}} \right) \cdot \left(\frac{\Delta h_{flame}}{h_v} \right) \cdot \frac{1.27 \cdot \left(\frac{\Delta h_{flame}}{h_v} \right)^{-0.77} \cdot C_{f_0}}{2} =$$

$$\frac{0.635}{P_r^{2/3}} \cdot \left(\frac{\Delta h_{flame}}{h_v} \right)^{0.23} \cdot \left(\frac{\rho_e \cdot U_e}{\rho_{fuel}} \right) C_{f_0}$$

Wall Blowing Correction ⁽⁶⁾

Allowing blowing-corrected skin friction to substitute for local skin friction coefficient "blowing adjusted" regression rate model

$$\dot{r} = \left(\frac{0.635}{P_r^{\frac{2}{3}}} \right) \left(\frac{\rho_e \cdot U_e}{\rho_{\text{fuel}}} \right) \left(\frac{\Delta h_{\text{flame}}}{h_f} \right)^{0.23} C_{f_0}$$

$C_{f_0} \rightarrow$ Skin Friction for Normal Boundary Layer Flow

Skin Friction Coefficient Model

- Blasius formula for turbulent wall shear stress

$$C_{f_x} = \frac{\tau_{wall_x}}{\frac{1}{2}\rho U_e^2} = \frac{0.0465}{(R_{e_x})^{1/4}} = \frac{0.0465}{\left(\frac{\rho U_e \delta_x}{\mu}\right)^{1/4}}$$

White, Frank M., *Viscous Fluid Flow*, McGrawHill, Inc., New York, 1991, pp. 485-486.

- Schoenherr-Schlichting Model for Turbulent Boundary Layer Thickness

$$\delta_x = \frac{0.38x}{(R_{e_x})^{1/5}} = \frac{0.38x}{\left(\frac{\rho U_e x}{\mu}\right)^{1/5}}$$

$$C_{f_x} = \frac{0.0465}{\left(\frac{\rho U_e \delta_x}{\mu}\right)^{1/5}} = \frac{0.0465 / (0.38)^{1/4}}{\left(\frac{\rho U_e x}{\mu} \frac{1}{\left(\frac{\rho U_e x}{\mu}\right)^{1/5}}\right)^{1/4}} = \frac{0.0592}{\left(\frac{\rho U_e x}{\mu}\right)^{1/5}}$$

Skin Friction Coefficient Model ⁽²⁾

- Substitute into Regression Rate Equation

$$C_{f_x} = \frac{0.0465}{\left(\frac{\rho U_e \delta_x}{\mu}\right)^{1/5}} = \frac{0.0465 / (0.38)^{1/4}}{\left(\frac{\rho U_e x}{\mu} \frac{1}{\left(\frac{\rho U_e x}{\mu}\right)^{1/5}}\right)^{1/4}} = \frac{0.0592}{\left(\frac{\rho U_e x}{\mu}\right)^{1/5}}$$

$$\dot{r} = \left(\frac{0.635}{P_r^{2/3}}\right) \left(\frac{\rho_e U_e}{\rho_{\text{fuel}}}\right) \left(\frac{\Delta h_{\text{flame}}}{h_f}\right)^{0.23} C_{f_0} = \left(\frac{0.635}{P_r^{2/3}}\right) \left(\frac{\rho_e U_e}{\rho_{\text{fuel}}}\right) \left(\frac{\Delta h_{\text{flame}}}{h_f}\right)^{0.23} \frac{0.0592}{\left(\frac{\rho_e U_e x}{\mu}\right)^{1/5}}$$

Skin Friction Coefficient Model ⁽²⁾

- Simplify Expression

Whew!

$$\dot{r} = \left(\frac{0.0376}{P_r^{2/3} \cdot \rho_{\text{fuel}}} \right) \left(\frac{\Delta h_{\text{flame}}}{h_f} \right)^{0.23} G_{ox}^{4/5} \cdot \left(\frac{\mu}{x} \right)^{1/5} \rightarrow G_{ox} = \frac{\dot{m}_{ox}}{A_c} = \rho_e U_e$$

- Compare to Original Marxman Correlation Equation

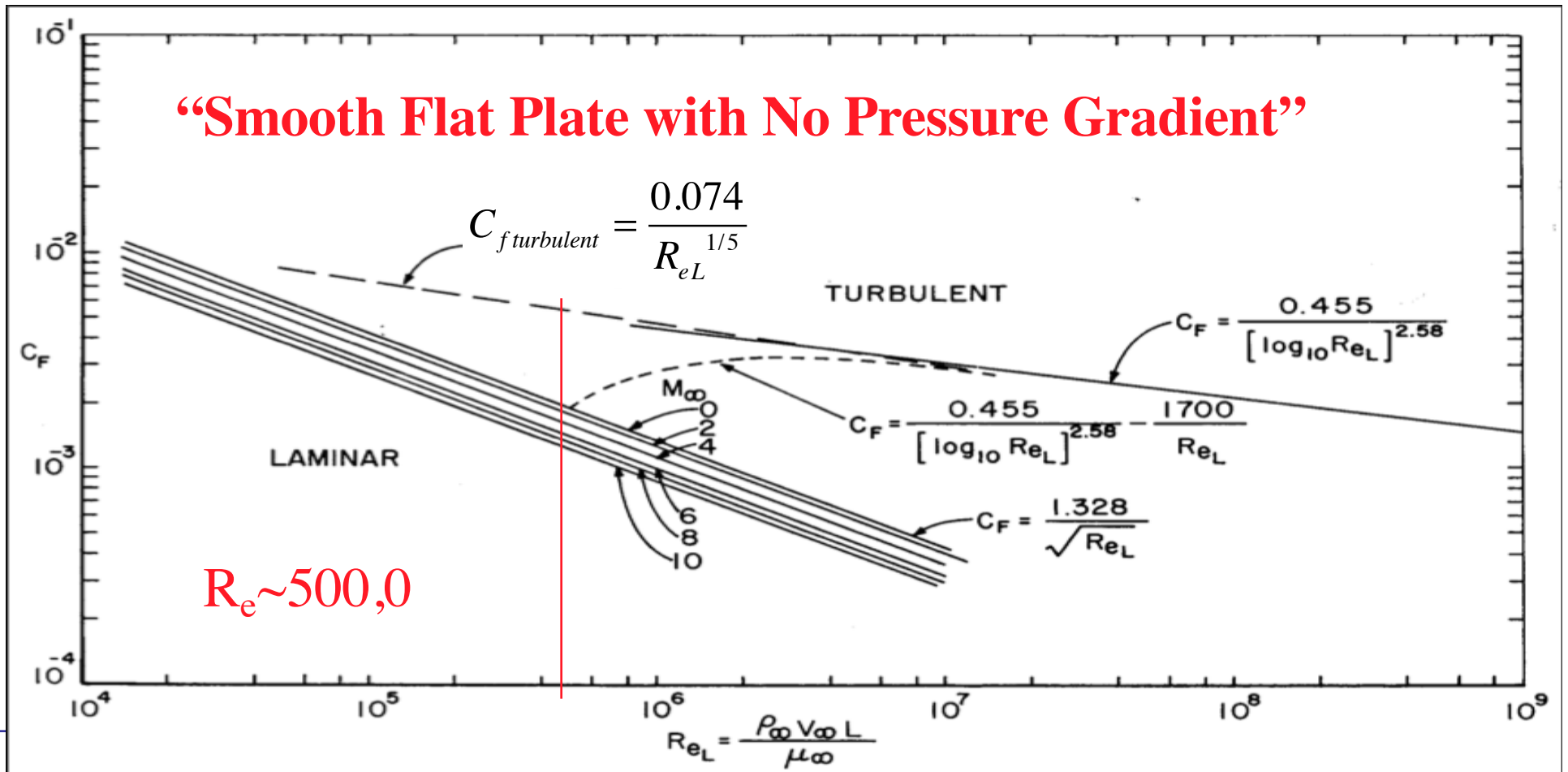
$$\dot{r} = \frac{.036}{\rho_f} \left(\frac{\mu_{\infty}}{x} \right)^{0.2} \frac{G^{0.8} B^{.23}}{\text{Pr}^{0.7}}$$

Very Close Comparisons and Based on First Principles

Longitudinally Averaged Regression Rate

- Mean Skin Friction Along Length of Port

$$C_{f_L} = \frac{1}{L} \cdot \int_0^L C_{f_x} \cdot dx = \frac{1}{L} \cdot \int_0^L \frac{0.0592}{\left(\frac{\rho_e U_e x}{\mu}\right)^{1/5}} \cdot dx = \frac{5}{4} \cdot \frac{1}{L} \cdot \frac{0.0592 \cdot L^{4/5}}{\left(\frac{\rho_e U_e}{\mu}\right)^{1/5}} = \frac{0.074}{(R_{e_L})^{1/5}}$$



Enthalpy Balance Regression Model Derivation (5)

- “Blowing corrected” regression rate model

$$\dot{r} = \left(\frac{0.635}{P_r^{2/3}} \right) \left(\frac{\rho_e \cdot U_e}{\rho_{fuel}} \right) \left(\frac{\Delta h_{flame}}{h_f} \right)^{0.23} C_{f_0}$$

Schlichting Flat-Plate
Turbulent Model

$$C_{f_0} = \frac{0.074}{[R_{e_L}]^{1/5}} \text{turbulent}$$

- Turbulent Flat Plate Skin Friction Model used to approximate $C_f \dots$

$$\begin{aligned} \dot{r} &= \frac{0.635}{P_r^{2/3}} \cdot \left(\frac{\Delta h_{flame}}{h_v} \right)^{0.23} \cdot \left(\frac{\rho_e \cdot U_e}{\rho_{fuel}} \right) \cdot \frac{0.074}{(R_{e_L})^{1/5}} = \\ &= \frac{0.047}{P_r^{2/3}} \cdot \left(\frac{\Delta h_{flame}}{h_v} \right)^{0.23} \cdot \left(\frac{\rho_e \cdot U_e}{\rho_{fuel}} \right) \cdot \frac{1}{\left(\frac{\rho_e \cdot U_e \cdot L}{\mu} \right)^{1/5}} = \\ &= \frac{0.047}{\rho_{fuel} \cdot P_r^{2/3}} \cdot \left(\frac{\Delta h_{flame}}{h_v} \right)^{0.23} \cdot (\rho_e \cdot U_e)^{4/5} \cdot \left(\frac{\mu}{L} \right) \end{aligned}$$

Enthalpy Balance Regression Model Derivation (6)

$$\dot{r} = \frac{0.047}{\rho_{fuel} \cdot P_r^{2/3}} \cdot \left(\frac{\Delta h_{flame}}{h_v} \right)^{0.23} \cdot (\rho_e \cdot U_e)^{4/5} \cdot \left(\frac{\mu}{L} \right)^{1/5}$$

• **Approximate massflux
at edge of Boundary
Layer as Oxidizer
Mass flux**

$$\rho_e U_e = \frac{\dot{m}_{ox}}{A_{c_{chamber}}} = G_{ox} \rightarrow A_{c_{chamber}} = \text{Instantaneous chamber cross-section}$$

$$\dot{r} = \frac{0.047}{P_r^{2/3} \cdot \rho_{fuel}} \cdot \left(\frac{\Delta h_{flame}}{h_v} \right)^{0.23} \cdot \left(\frac{\dot{m}_{ox}}{A_c} \right)^{4/5} \cdot \left(\frac{\mu_e}{L} \right)^{1/5} =$$

$$\frac{0.047}{\rho_{fuel} \cdot P_r^{2/3}} \cdot \left(\frac{C_{P_e} \cdot (T_{flame} - T_{fuel_{surf}})}{h_{v_{fuel_{surf}}}} \right)^{0.23} \cdot \left(\frac{\dot{m}_{ox}}{A_c} \right)^{4/5} \cdot \left(\frac{\mu_e}{L} \right)^{1/5}$$

Enthalpy Balance Model Derivation ⁽³⁾

- Substituting in the Incompressible Discharge formula for Injector Mass-flow

$$\dot{m}_{ox} = (C_d \cdot A_{inj})_{ox} \cdot \sqrt{2 \cdot \rho_{ox} \cdot \left(P_{inj_{ox}} - P_{0_{chamber}} \right)}$$

Longitudinally Averaged skin friction Coefficient ... “whole motor”

- *Longitudinally averaged regression rate*

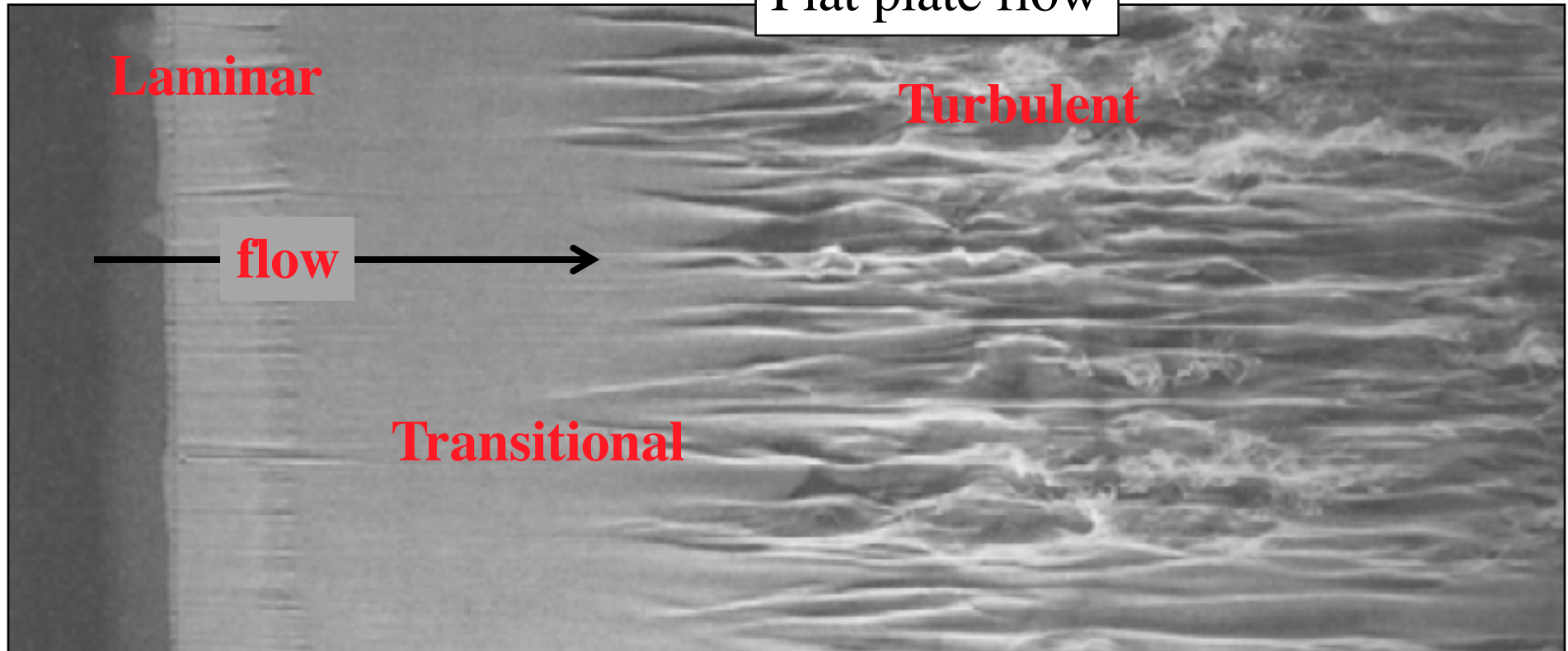
$$\dot{r} = \frac{0.047}{\rho_{fuel} \cdot P_r^{2/3}} \cdot \left(\frac{C_{P_e} \cdot \left(T_{flame} - T_{fuel_{surf}} \right)}{h_{v_{fuel_{surf}}}} \right)^{0.23} \cdot \left(\frac{C_d \cdot A_{inj} \cdot \sqrt{2 \cdot \rho_{ox} \cdot \left(P_{inj_{ox}} - P_{0_{chamber}} \right)}}{A_c} \right)^{4/5} \cdot \left(\frac{\mu_e}{L} \right)^{1/5}$$

- Model derived in a form suitable for easy integration.
- Result is nearly identical to Marxman and Gilbert correlation model

How Do We Justify a “Flat Plate” Skin Friction Model?

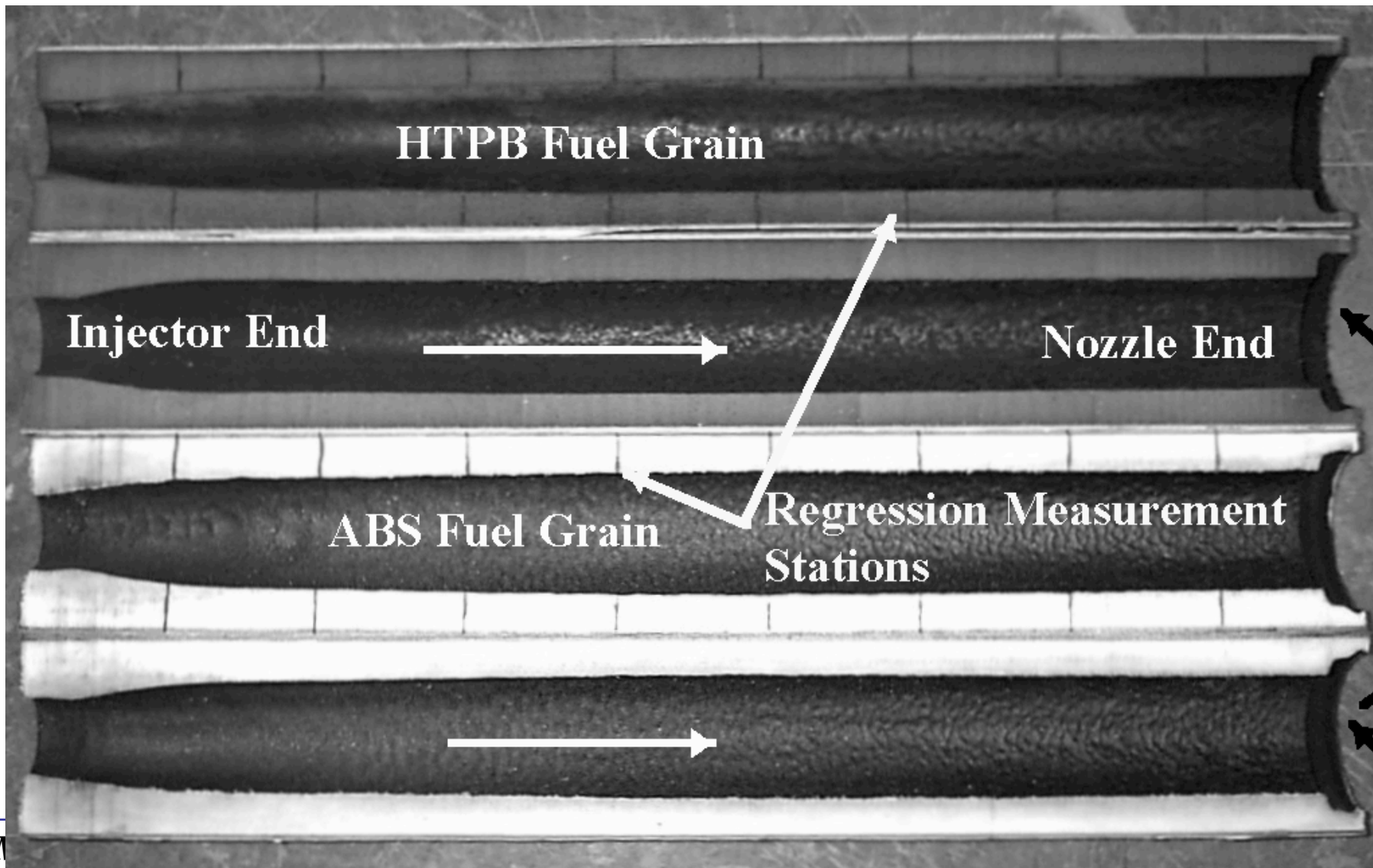
... Look at the evidence?

Flat plate flow

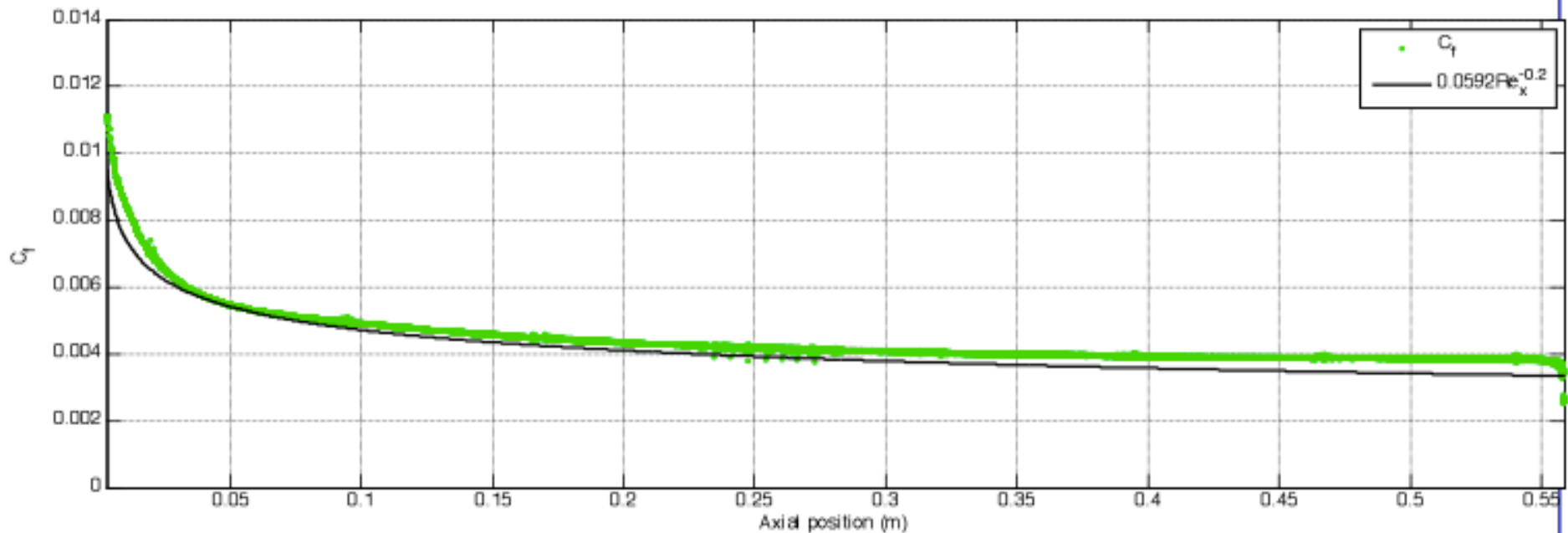


How Do We Justify a “Flat Plate” Skin Friction Model?

... Look at the evidence? (2)



How Do We Justify a “Flat Plate” Skin Friction Model?



Evolving pipe flow with radial injection skin friction shear stress coefficient compared to turbulent flat plate profile

Regression Rate Equation Examined

- Heat transfer related through oxidizer mass velocity and Stanton number

Resulting Heat Transfer From Reynolds Number

$$\dot{r} = \frac{0.047}{\rho_{fuel} \cdot P_r^{2/3}} \cdot \left(\frac{C_{P_e} \cdot (T_{flame} - T_{fuel\ surf})}{h_{v\ fuel\ surf}} \right)^{0.23} \cdot \left(\frac{C_d \cdot A_{inj} \cdot \sqrt{2 \cdot \rho_{ox} \cdot (p_{inj\ ox} - P_{0\ chamber})}}{A_c} \right)^{4/5} \cdot \left(\frac{\mu_e}{L} \right)^{1/5}$$

- Result is, in turn, related to the Prandtl number and the skin friction coefficient

Oxidizer Mass Velocity Term (G_{ox})

$$n \approx 4 / 5$$

$$\left\{ \rho_{fuel}, T_{solid\ fuel}, (h_v)_{solid\ fuel} \right\} \rightarrow \text{solid phase fuel properties}$$

ρ_{ox} → density of liquid phase oxidizer

$\{C_{pe}, \mu_e, P_r\}$ → Specific heat, Viscosity, Prandtl number of combustion products at flame temperature

Generic form of model

$$\dot{r}_L = a \cdot G_{ox}^n \cdot L^m$$

Instantaneous mixture (O/F) ratio

$$M_{O/F} = \frac{\dot{m}_{ox}}{\dot{m}_{fuel}} = \frac{\dot{m}_{ox}}{\rho_{fuel} \cdot A_{burn} \cdot \dot{r}_{fuel}} =$$

$$\frac{\dot{m}_{ox}}{\rho_{fuel} \cdot A_{burn} \cdot \frac{0.047}{\rho_{fuel} \cdot P_r^{2/3}} \cdot \left(\frac{\Delta h_{flame\ fuel}}{h_{v\ solid\ fuel}} \right)^{0.23} \cdot \left(\frac{\dot{m}_{ox}}{A_{c\ port}} \right)^{4/5} \cdot \left(\frac{\mu_e}{L} \right)^{1/5}} =$$

$$21.2766 \cdot P_r^{2/3} \cdot \left(\frac{h_{v\ solid\ fuel}}{\Delta h_{flame\ fuel}} \right)^{0.23} \cdot \frac{(\dot{m}_{ox})^{1/5} \cdot \left(\frac{A_{c\ port}}{A_{burn}} \right)^{4/5}}{\left(A_{burn} \cdot \frac{\mu_e}{L} \right)^{1/5}}$$

- O/F ratio is independent of Fuel density ...
..... why ?

Instantaneous mixture (O/F) ratio (2)

for near-cylindrical port \rightarrow

$$\boxed{\begin{aligned} A_{burn} &= \pi \cdot D \cdot L \\ A_{c\ chamber} &= \frac{\pi}{4} D^2 \end{aligned}}$$

$$M_{O/F} = 21.2766 \cdot P_r^{2/3} \cdot \left(\frac{h_{v\ solid\ fuel}}{\Delta h_{flame\ fuel}} \right)^{0.23} \cdot (\dot{m}_{ox})^{1/5} \cdot \frac{\left(\frac{\pi \cdot D^2}{4 \cdot \pi \cdot D \cdot L} \right)^{4/5}}{\left(\pi \cdot D \cdot L \cdot \frac{\mu_e}{L} \right)^{1/5}} =$$

$$21.2766 \cdot P_r^{2/3} \cdot \left(\frac{h_{v\ solid\ fuel}}{\Delta h_{flame\ fuel}} \right)^{0.23} \cdot \left(\frac{\dot{m}_{ox}}{\mu_e} \right)^{1/5} \cdot \frac{\left(\frac{D}{4 \cdot L} \right)^{4/5}}{(\pi \cdot D)^{1/5}} = \frac{21.2766}{(256 \cdot \pi)^{1/5}} \cdot P_r^{2/3} \cdot \left(\frac{h_{v\ solid\ fuel}}{\Delta h_{flame\ fuel}} \right)^{0.23} \cdot \left(\frac{\dot{m}_{ox}}{\mu_e} \right)^{1/5} \cdot \frac{D^{3/5}}{L^{4/5}}$$

$$5.58244 \cdot P_r^{2/3} \cdot \left(\frac{h_{v\ solid\ fuel}}{\Delta h_{flame\ fuel}} \right)^{0.23} \cdot \left(\frac{\dot{m}_{ox}}{\mu_e \cdot L} \right)^{1/5} \left(\frac{D}{L} \right)^{3/5}$$

Instantaneous mixture (O/F) ratio ⁽³⁾

for near-cylindrical port \rightarrow

$$\begin{array}{l} A_{burn} = \pi \cdot D \cdot L \\ A_{c\ chamber} = \frac{\pi}{4} D^2 \end{array}$$

As motor burns ... $D = D_0 + 2 \int_0^r \dot{r} \cdot dt$

$$M_{O/F}(t) = 5.58244 \cdot P_r^{2/3} \cdot \left(\frac{h_{v\ solid\ fuel}}{\Delta h_{flame\ fuel}} \right)^{0.23} \cdot \left(\frac{\dot{m}_{ox}}{\mu_e \cdot L} \right)^{1/5} \left(\frac{D_0 + 2 \cdot \int_0^t \dot{r}(\tau) \cdot d\tau}{L} \right)^{3/5}$$

O/F positive shift is inherent to hybrid rockets with cylindrical port, And in general over the course of a burn at a fixed oxidizer mass flow rate there is a tendency for the oxidizer to fuel (O/F) ratio to shift to higher values as the port opens up.

Instantaneous mixture (O/F) ratio (4)

for near-cylindrical port \rightarrow

$$\begin{aligned} A_{burn} &= \pi \cdot D \cdot L \\ A_{c\ chamber} &= \frac{\pi}{4} D^2 \end{aligned}$$

In terms of generic model... $\dot{r}_x = a \cdot G_{ox}^n \cdot x^m \approx a \cdot G_{ox}^n \cdot x^{1-n}$

$$\begin{aligned} O/F &= \frac{\dot{m}_{ox}}{\dot{m}_{fuel}} = \frac{\dot{m}_{ox}}{\rho_{fuel} \cdot (2 \cdot \pi \cdot r_L \cdot L) \cdot \dot{r}_L} = \frac{\dot{m}_{ox}}{\rho_{fuel} \cdot (\pi \cdot D_{port} \cdot L) \cdot a \cdot G_{ox}^n \cdot L^m} = \\ &= \frac{\dot{m}_{ox}}{\rho_{fuel} \cdot (\pi \cdot D_{port} \cdot L) \cdot a \cdot \left(\frac{4 \cdot \dot{m}_{ox}}{\pi \cdot D_{port}^2} \right)^n \cdot L^{1-n}} = \frac{1}{4^n \cdot \pi^{1-n}} \frac{\dot{m}_{ox}^{1-n} \cdot D_{port}^{2n-1}}{a \cdot \rho_{fuel} \cdot L^{1-n}} \end{aligned}$$

$n = 1/2 \rightarrow$ No O/F shift !

Instantaneous mixture (O/F) ratio ⁽⁵⁾

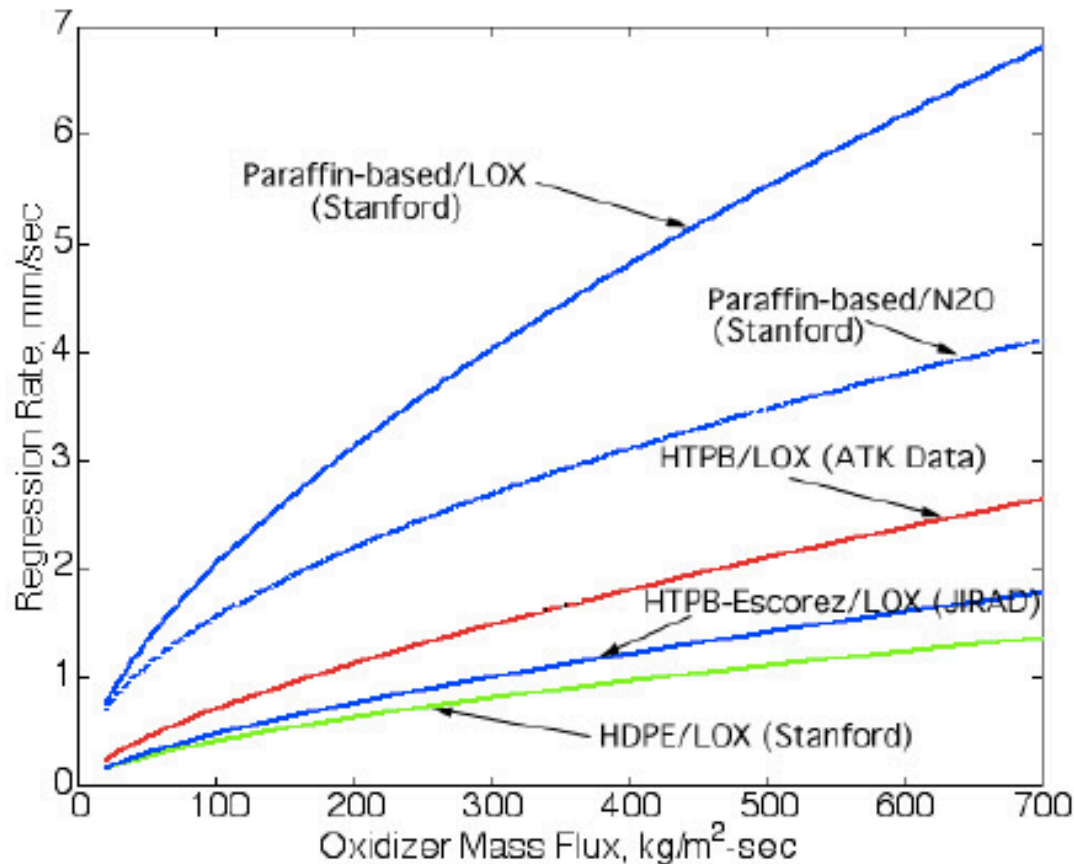
Consequences of O/F shift

- ... reduced motor performance
- ... potential for combustion instability
- ... nozzle or port erosion
- ... decreased duty cycle lifetime
- ... More oxidizer (typically least volumetric efficient component) required

$n = \frac{1}{2} \rightarrow$ No O/F shift !

Instantaneous mixture (O/F) ratio ⁽⁶⁾

Regression Rate Data for Various Hybrid Propellants



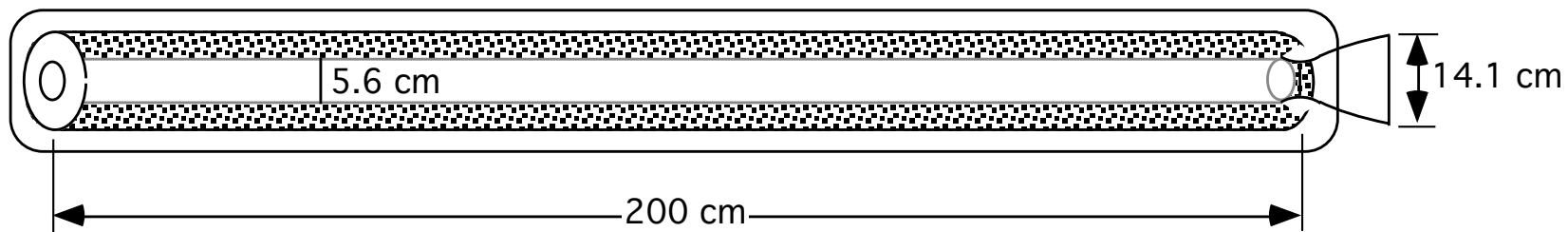
- **HTPB/LOX:**
 $\dot{r} = 3.043 \cdot 10^{-2} G_{ox}^{0.681}$
- **HTPB/Escorez/LOX**
 $\dot{r} = 2.061 \cdot 10^{-2} G_{ox}^{0.68}$
- **HDPE/LOX**
 $\dot{r} = 2.340 \cdot 10^{-2} G_{ox}^{0.62}$
- **Paraffin/LOX**
 $\dot{r} = 11.70 \cdot 10^{-2} G_{ox}^{0.62}$
- **Paraffin/N2O**
 $\dot{r} = 15.50 \cdot 10^{-2} G_{ox}^{0.50}$

(Units are mm/sec and kg/m²-sec)

Example Calculation

LOX/ HTPB Hybrid Numerical Example

- Design Hybrid Rocket Motor, Nominal Thrust 8.4 kNt
- Approximate Dimensions Below
- LOX/HTPB Propellants, Operate Near Optimal O/F Ratio
- Cylindrical Grain Pattern, Initial Diameter, 5.6 cm
- Nozzle Throat Diameter, 4.98 cm
- Nozzle $A/A^* = 8.0$



LOX/ HTPB Hybrid Numerical Example (cont'd)

- Combustion Properties

NASA CEA (chemical equilibrium with applications)

–NASA Reference Publication 1311 (June 1996)

CEA can be obtained for free

–<http://www.grc.nasa.gov/WWW/CEAWeb/>

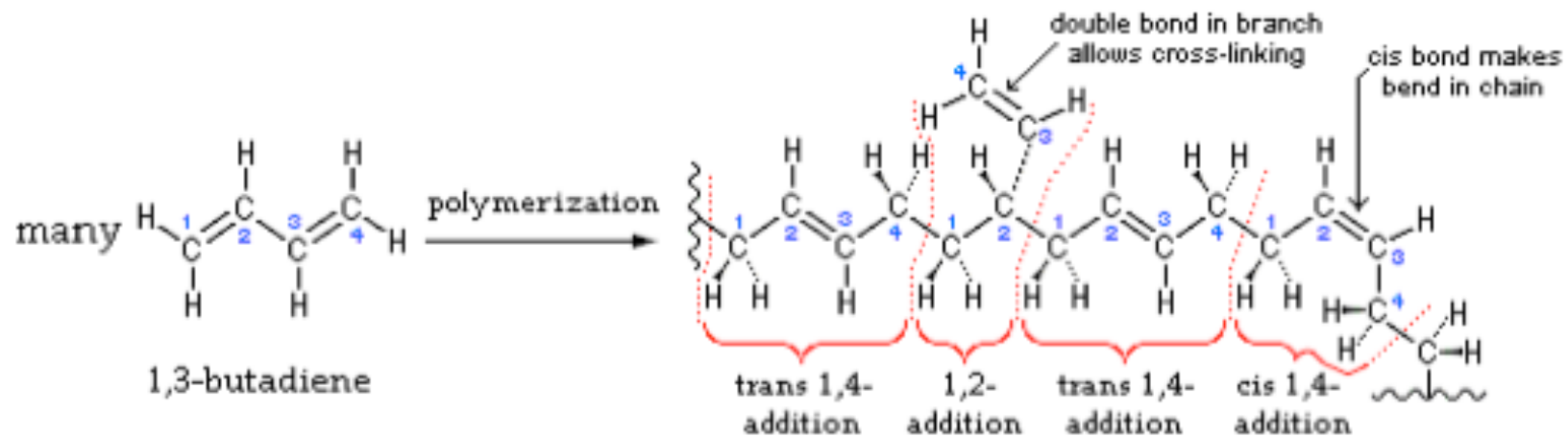
Sample CEA Calculation

HTPB ... solid form $(C_4H_6)_n(OH)_2$

... A hydrocarbon butadiene molecule has two C=C double bonds

... Polybutadiene is a synthetic rubber that has a high resistance to wear and is used especially in the manufacture of tires.

... Polybutadiene can be formed from many 1,3-butadiene monomers radical polymerization to make a much longer undergoing free polymer chain molecule.



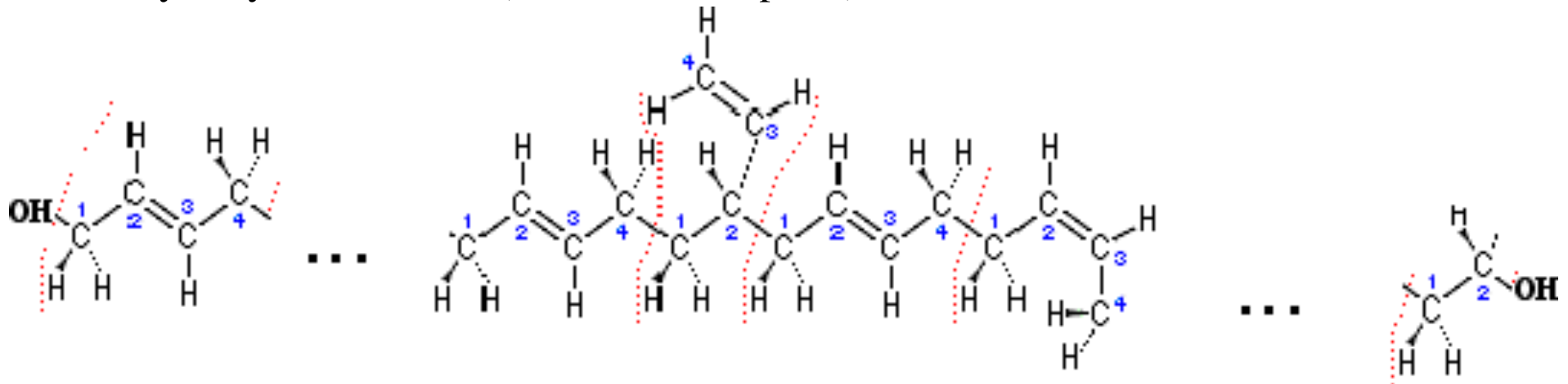
Sample CEA Calculation (cont'd)

- Example for 8:5 to one Mixture ratio, Nitrous Oxide + HTPB

HTPB ... solid form $(C_4H_6)_n(OH)_2$

Hydroxy-terminated polybutadiene (HTPB) is a polymer of butadiene terminated at each end with a hydroxyl functional group

The effect is increased functionality of the polybutadiene on mechanical properties, thermal behavior (*lower glassification* or *embrittlement* temperature) and hydrolytic resistance (moisture absorption).



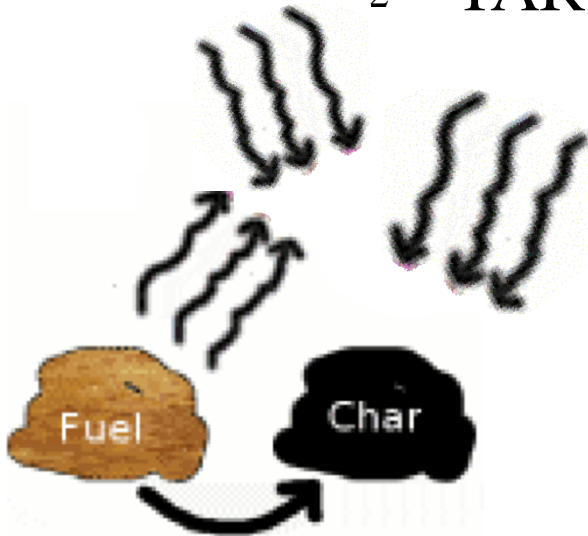
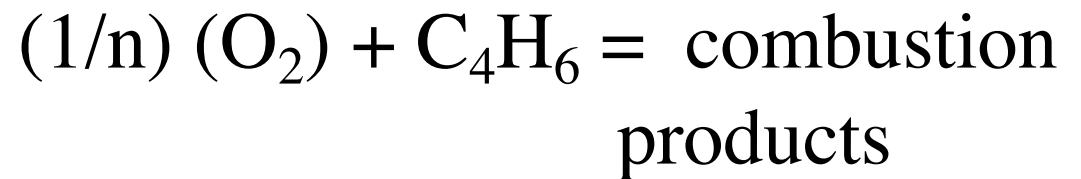
Sample CEA Calculation (cont'd)

- When HTPB undergoes decomposition ... that is ... it is Baked off from the solid grain core ...



- Main “fuel” for combustion reaction

C_4H_6 (butadiene gas)
 O_2 H_2 TARs



APPROXIMATE ANALYSIS

LOX/ HTPB Hybrid Numerical Example (cont'd)

- Sample CEA Computation

$$M_{O/F} = \frac{\dot{m}_{O_2}}{\dot{m}_{C_4H_6}} \rightarrow \left[\begin{array}{l} \text{moles}_{O_2} = \frac{\dot{m}_{O_2}}{M_{W_{O_2}}} \\ \text{moles}_{C_4H_6} = \frac{\dot{m}_{C_4H_6}}{M_{W_{C_4H_6}}} \end{array} \right] \rightarrow$$

$$\frac{\text{moles}_{O_2}}{\text{moles}_{C_4H_6}} = \frac{\dot{m}_{O_2}}{M_{W_{O_2}}} \times \frac{M_{W_{C_4H_6}}}{\dot{m}_{C_4H_6}} = M_R \times \frac{\dot{m}_{C_4H_6}}{M_{W_{O_2}}} \times \frac{M_{W_{C_4H_6}}}{\dot{m}_{C_4H_6}} =$$

$$M_{O/F} M_R \times \frac{M_{W_{C_4H_6}}}{M_{W_{O_2}}} \approx M_R \times \frac{4 \times 12 + 6}{2 \times 16} = 1.687 M_{O/F}$$

LOX/ HTPB Hybrid Numerical Example (cont'd)

- Sample CEA Computation Look at O/F Ratio of 2.5

$$\frac{\text{moles}_{O_2}}{\text{moles}_{C_4H_6}} = 1.6875 \times 2.5 \rightarrow 4.21875 O_2 + C_4H_6 \rightarrow$$

Combustion Product Mole fractions

CO	0.35492
CO2	0.15747
COOH	0.002
H	0.03513
HCO	0.003
HO2	0.012
H2	0.06871
H2O	0.26134
H2O2	0.001
O	0.02002
OH	0.07323
O2	0.02900

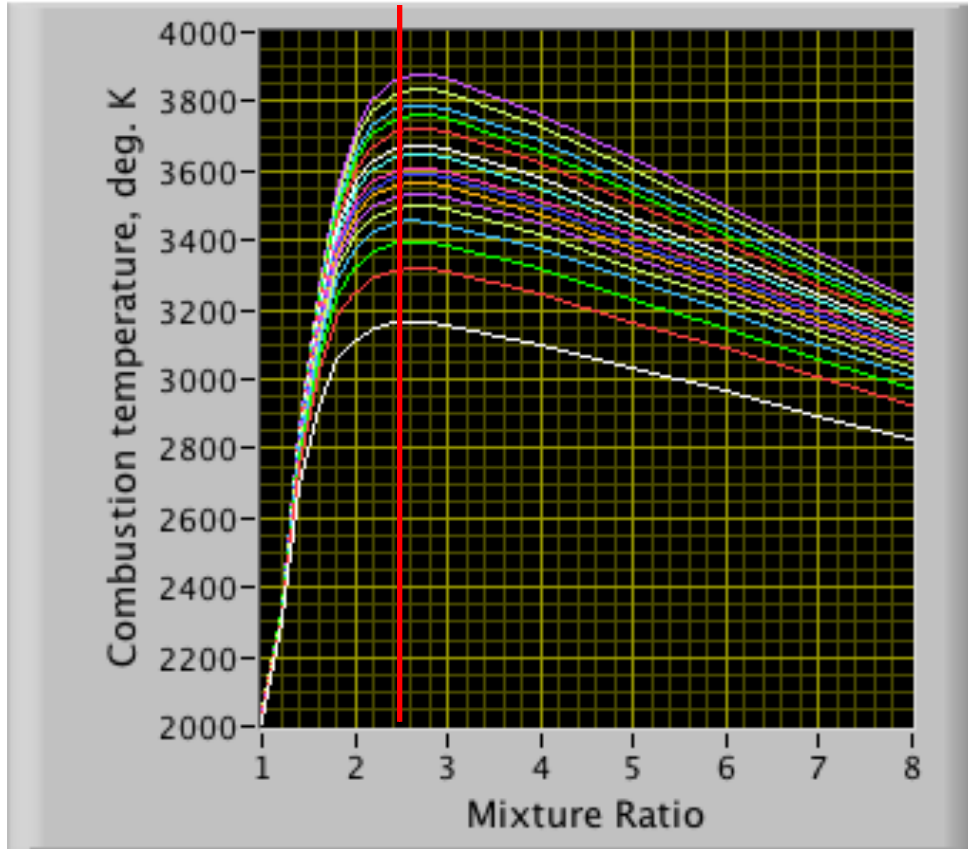
- Mean Exhaust Gas Properties:

$$\begin{aligned} \gamma &= 1.1362 \\ C^* &= 1775.7 \text{ m/sec} \\ M_w &= 24.253 \end{aligned}$$

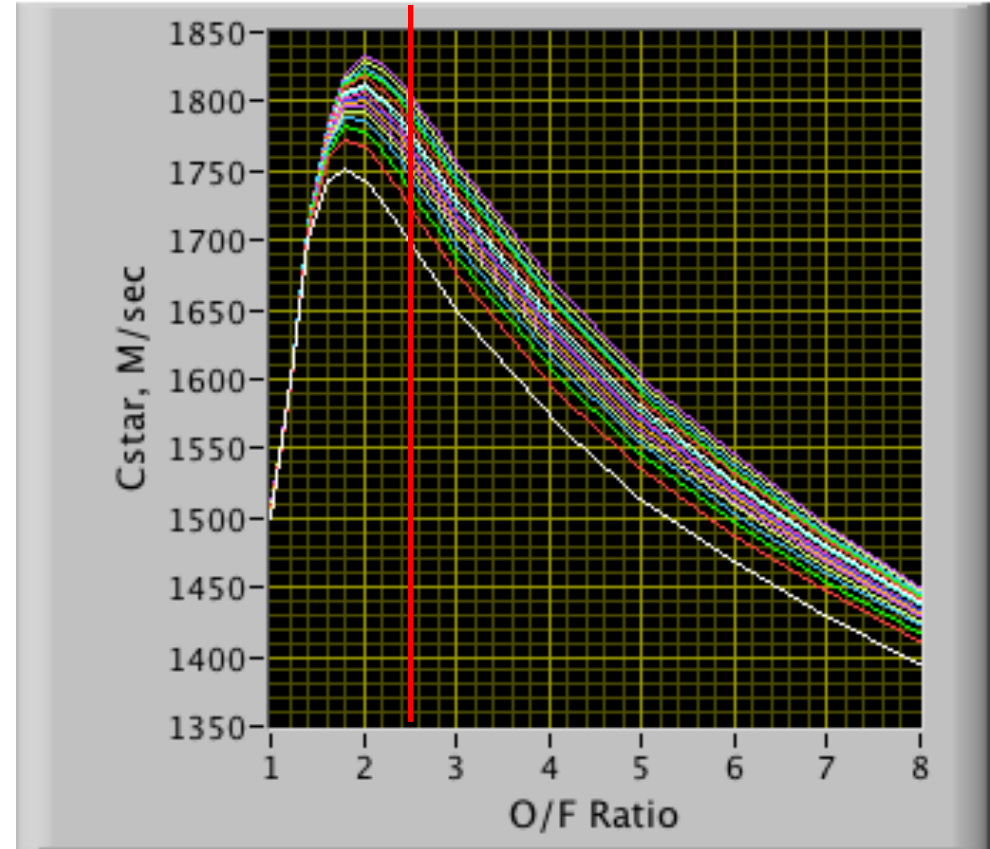
Sample CEA Calculation (cont'd)

LOX/HTPB as Function of Mean O/F

T0



Cstar

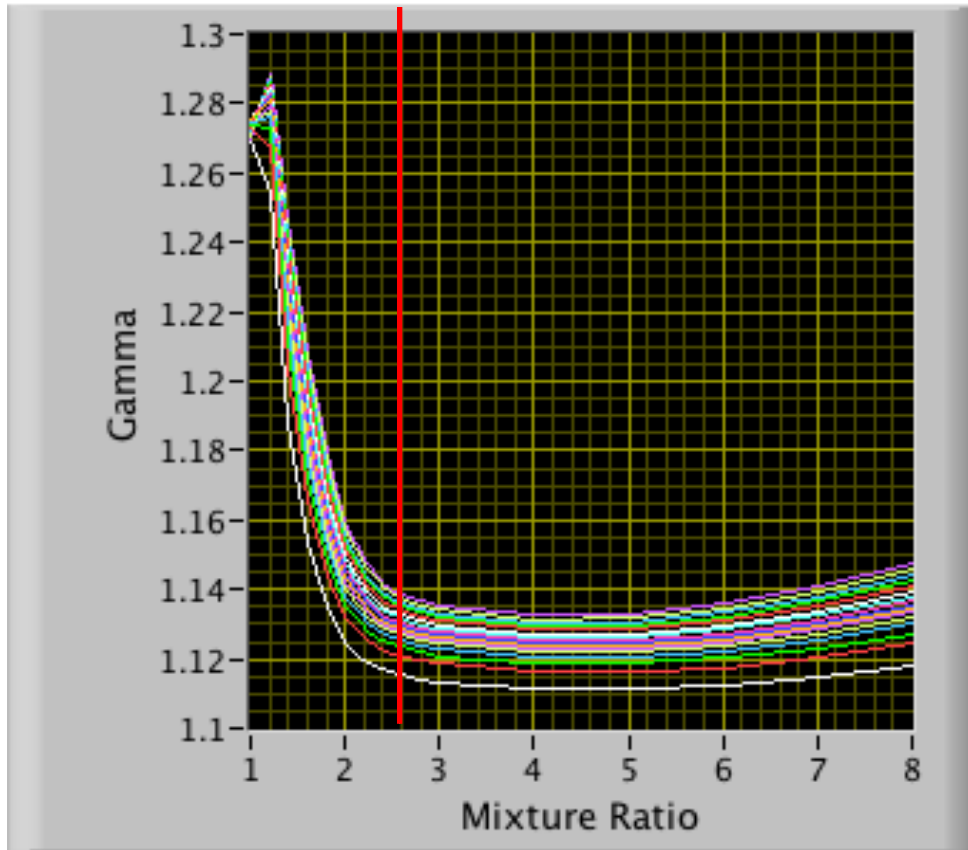


Stoichiometric O/F near 2.5 Best Cstar O/F Ratio Near 2.0

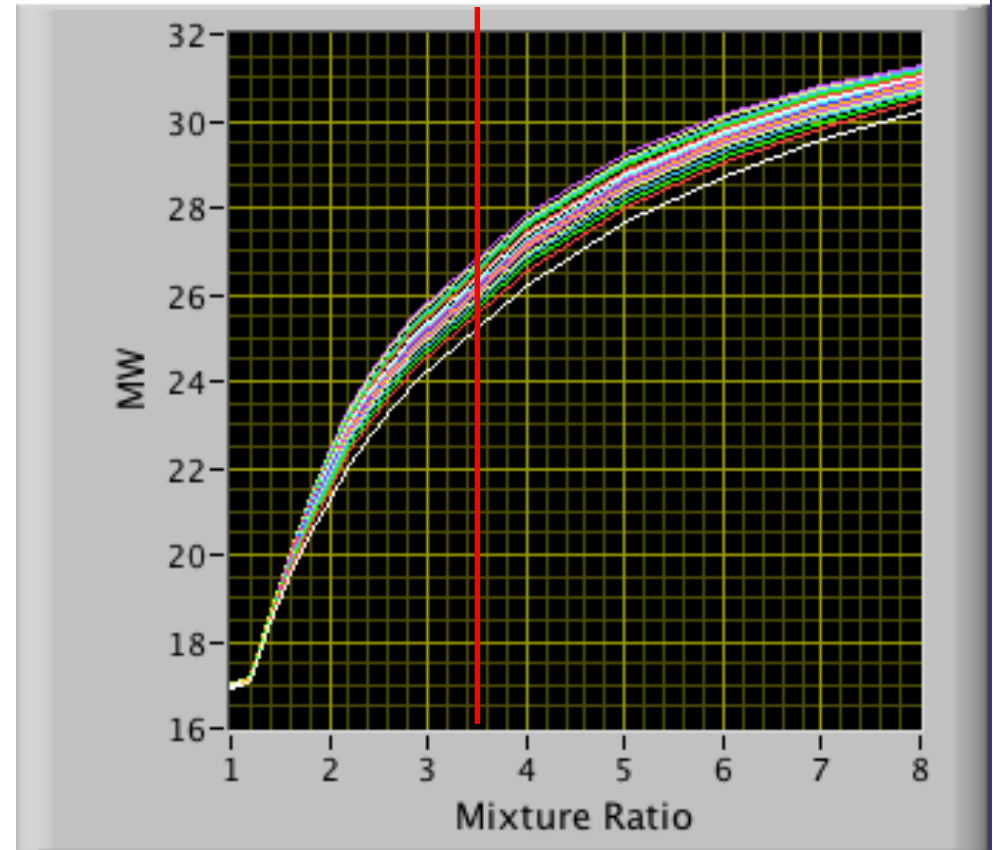
Sample CEA Calculation (cont'd)

LOX/HTPB as Function of Mean O/F

Gamma



MW

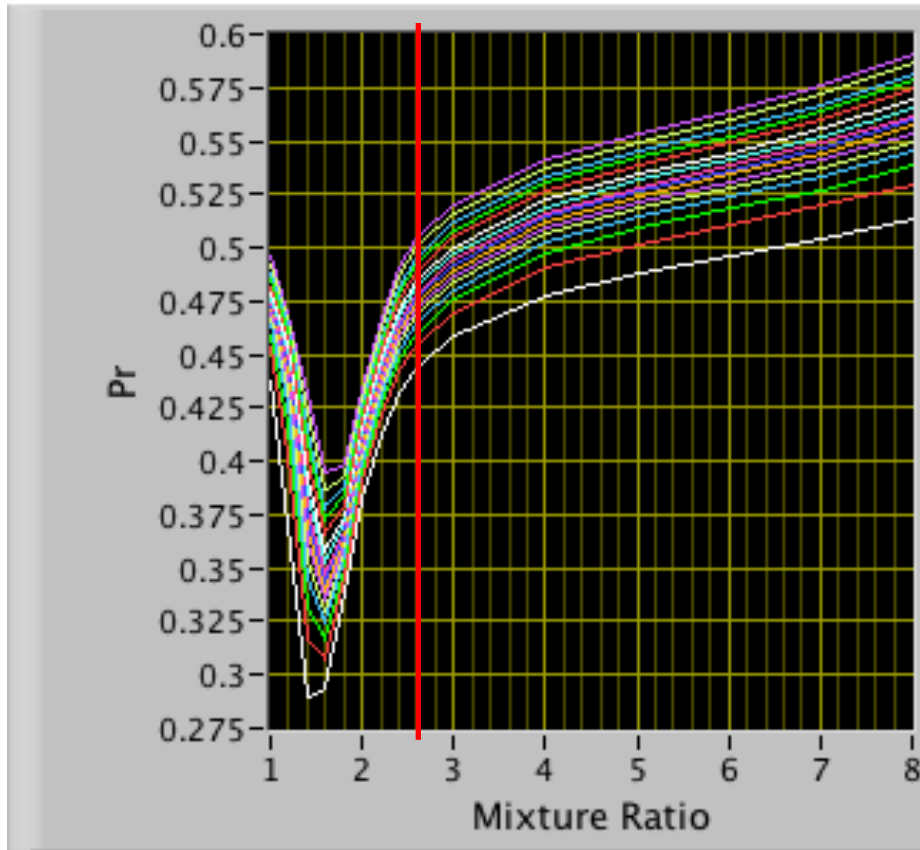


Best O/F Ratio Near 2.0

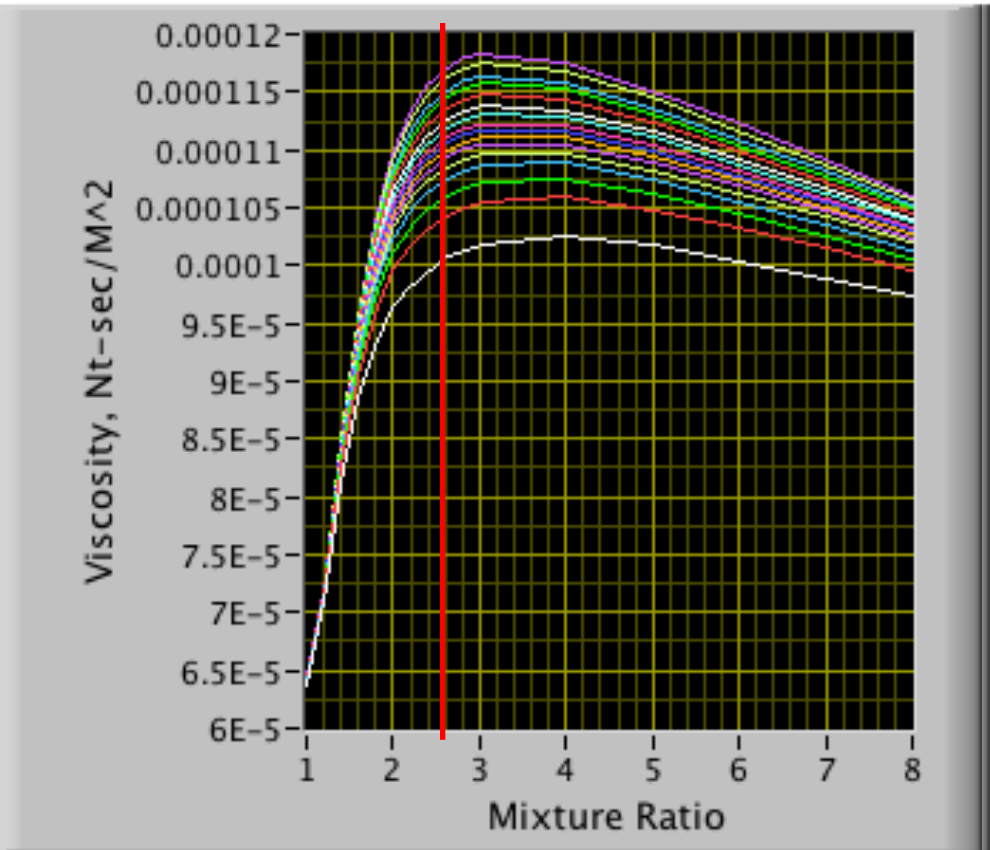
Sample CEA Calculation (cont'd)

LOX/HTPB as Function of Mean O/F

Prandtl Number



Viscosity



Best O/F Ratio Near 2.0

LOX/ HTPB Hybrid Numerical Example (cont'd)

- Problem parameters

LOX/Injector Properties

Injector Area, cm²

Injector Discharge Coefficient

Oxydizer Liquid Density, kg/M³

Oxydizer Injector Pressure, kPa

Total Oxydizer mass, kg

Nozzle Characteristics

A/A*

Throat Area, M²

Nozzle exit divergence angle, deg

HTPB / Fuel grain Properties

PROPELLANT DENSITY KG/M³

LENGTH, M

INSIDE Hydraulic DIAMETER, M

Grain temperature , deg K

Heat of Vaporization, MJ/kg

Total Fuel mass, kg

Burn Area Rate reduction factor

Iteration control

Max Iterations

Convergence error %

COMBUSTION EFFICIENCY, (C*/C*ideal)

T0, Initial deg K

Mixture ratio, Initial

Default Prandtl Number

Ambient Pressure kPa

LOX/ HTPB Hybrid Numerical Example (cont'd)

• State Equations

$$\frac{\partial P_0}{\partial t} = \frac{A_{burn} \dot{r}_{fuel}}{V_c} [\rho_{fuel} R_g T_0 - P_0] - P_0 \left[\frac{A_{burn}}{V_c} \sqrt{\gamma R_g T_0 \left(\frac{2}{\gamma + 1} \right)^{\frac{\gamma+1}{\gamma-1}}} \right] + \frac{R_g T_0}{V_c} A_{ox} C_{d_{ox}} \sqrt{2 \rho_{ox} (p_{ox} - P_0)}$$

$$\frac{\partial R_{chamber}}{\partial t} = \dot{r}_{fuel}$$

$$\frac{\partial M_{LOX}}{\partial t} = A_{ox} C_{d_{ox}} \sqrt{2 \rho_{ox} (p_{ox} - P_0)}$$

$$\frac{\partial M_{HTPB}}{\partial t} = \rho_{fuel} A_{burn} \dot{r}_{fuel}$$

• Port Cross Section and Volume

$$\left[\begin{array}{l} A_{burn} = 2\pi R_{chamber} L_{prop} \\ V_c = \pi R_{chamber}^2 L_{prop} \end{array} \right]$$

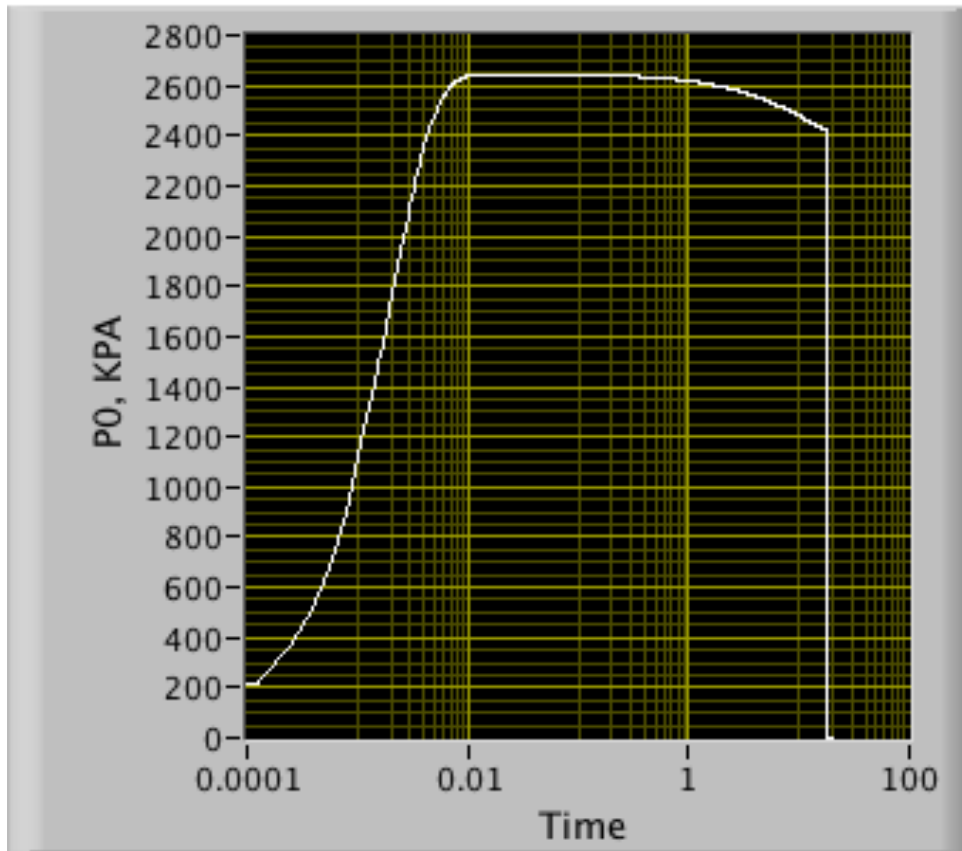
$$\left[\begin{array}{l} P_0 \\ R_{chamber} \\ M_{LOX} \\ M_{HTPB} \end{array} \right]$$

• Port Regression Rate

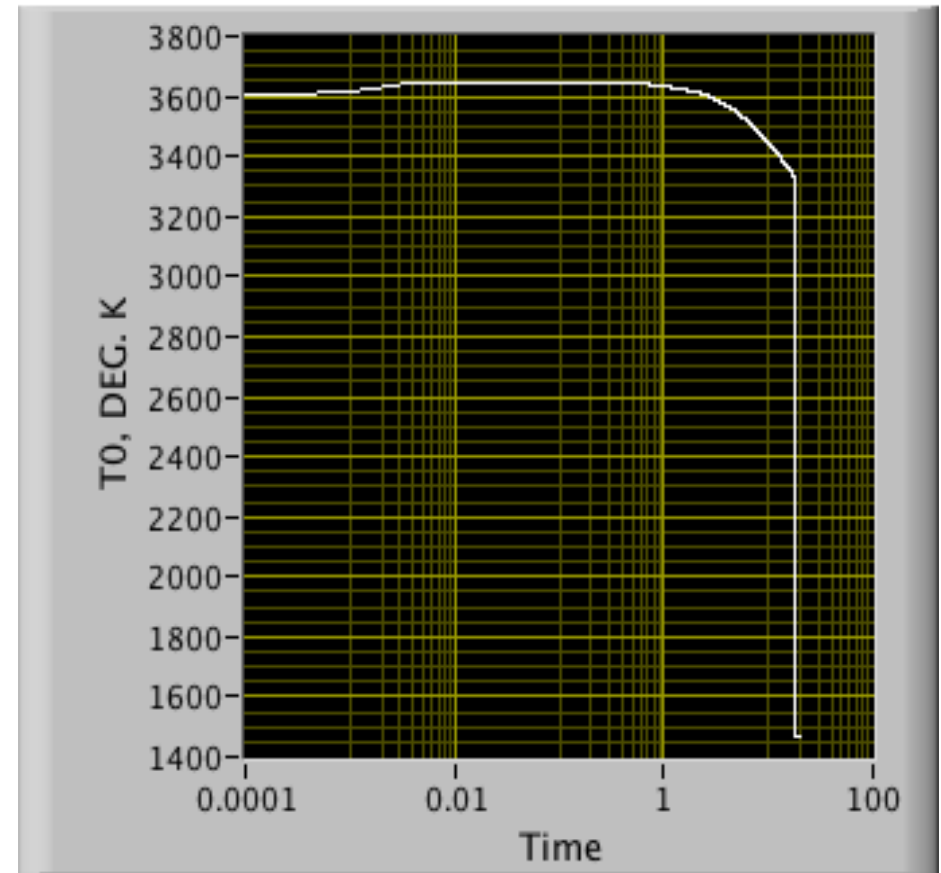
$$\dot{r} = \left(\frac{0.0376}{P_r^{2/3} \cdot \rho_{fuel}} \right) \left(\frac{\Delta h_{flame}}{h_f} \right)^{0.23} G_{ox}^{4/5} \cdot \left(\frac{\mu}{x} \right)^{1/5}$$

LOX/ HTPB Hybrid Numerical Example (cont'd)

BURNER PRESSURE

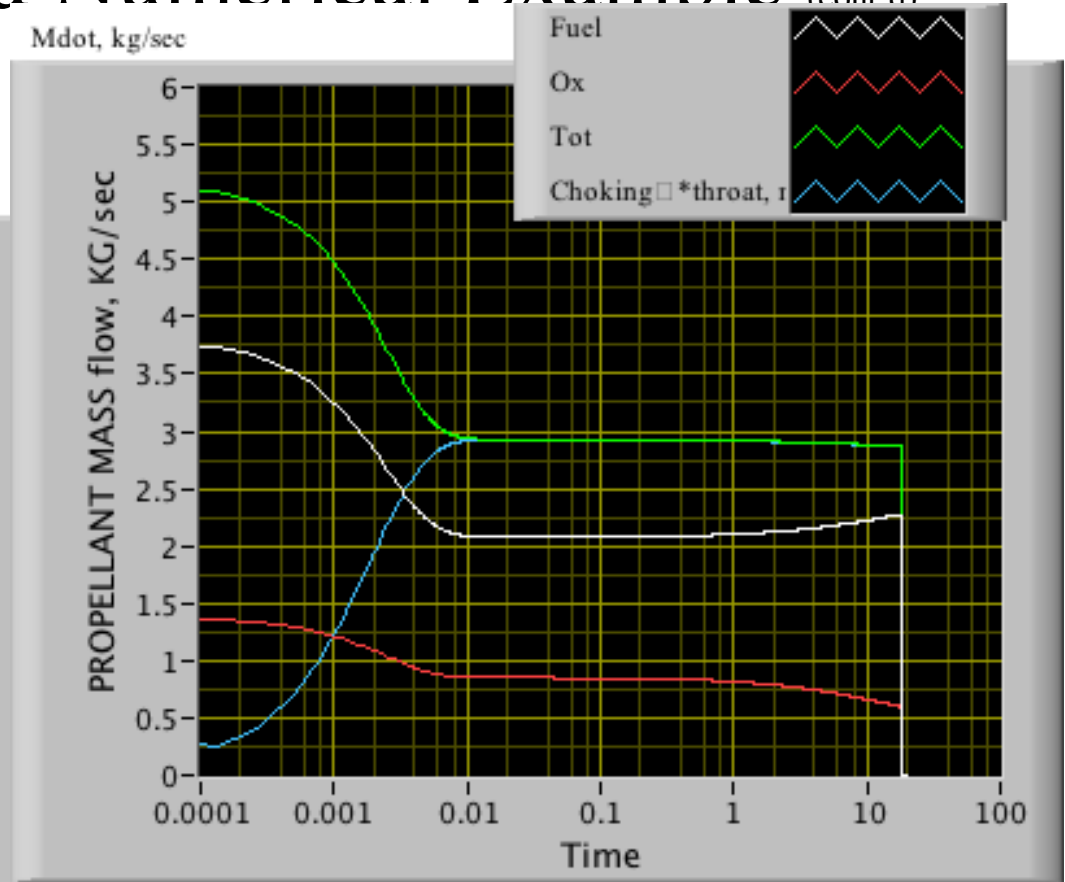
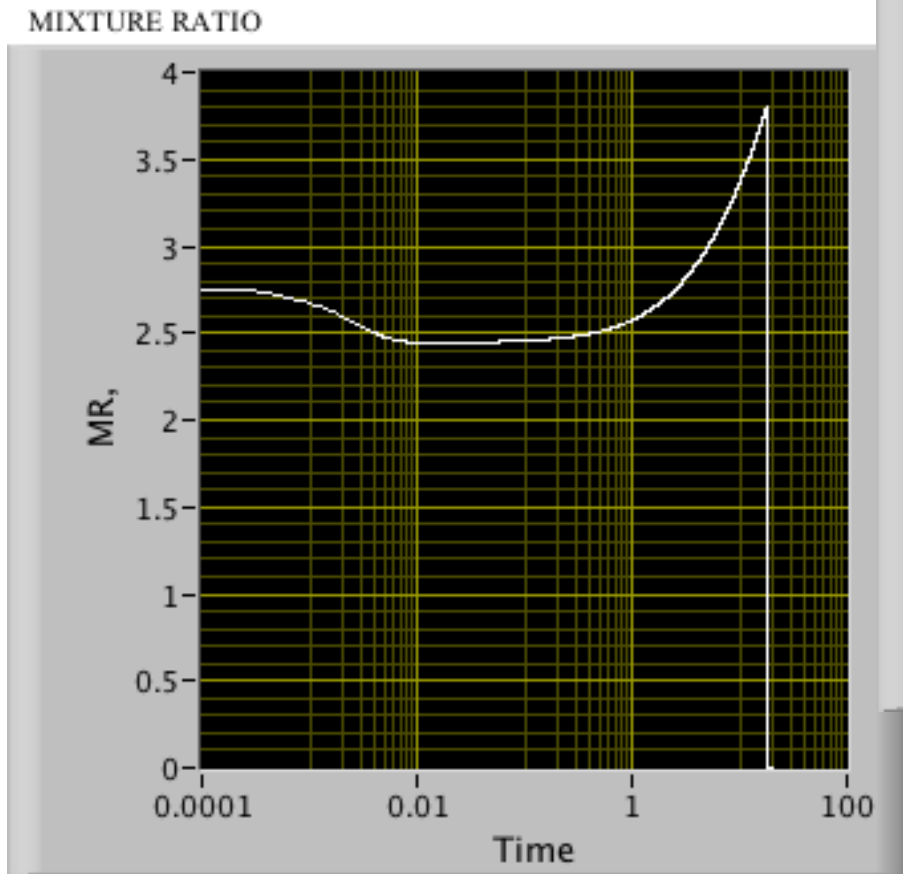


BURNER TEMPERATURE



- Burn Time ~ 18 seconds

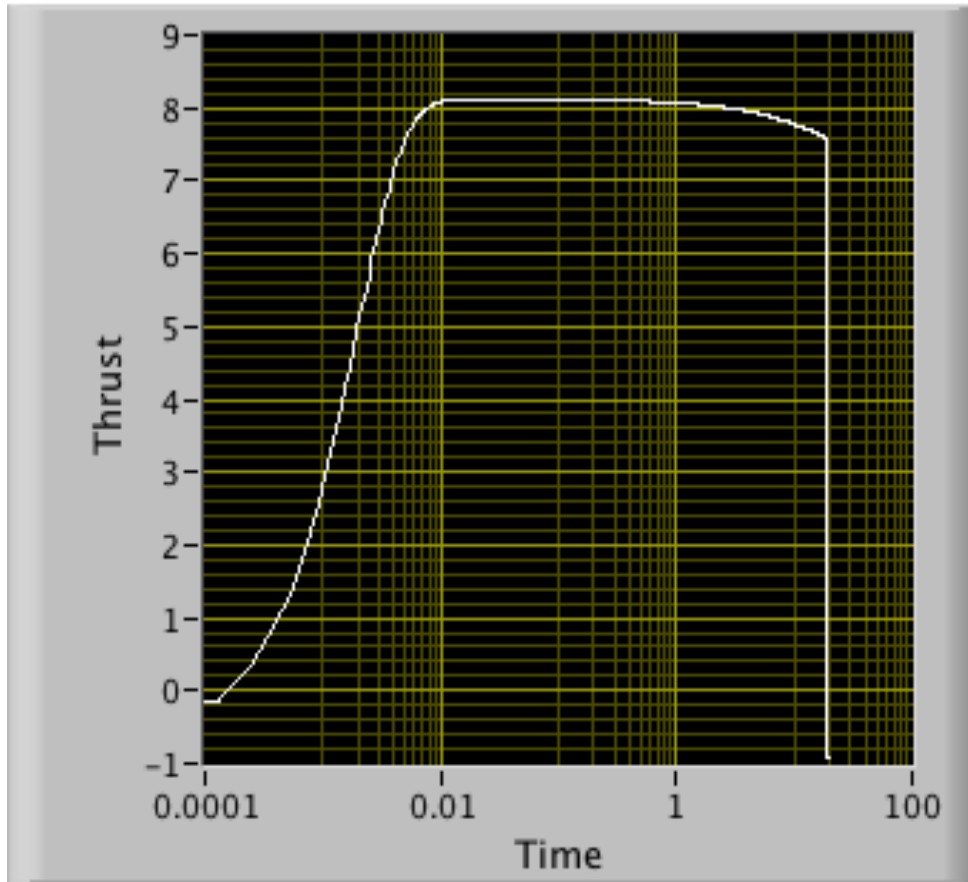
LOX/ HTPPB Hybrid Numerical Example (cont'd)



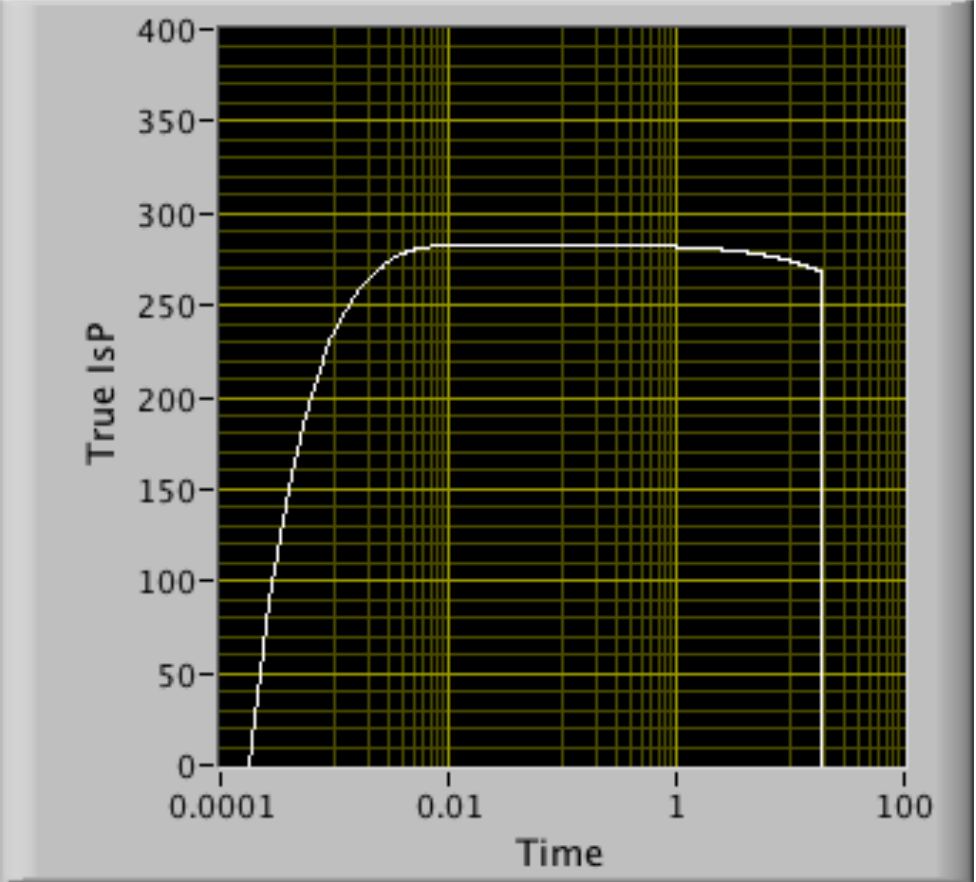
Notice distinct O/F shift

LOX/ HTPB Hybrid Numerical Example (cont'd)

Thrust, kN



Specific Impulse, sec

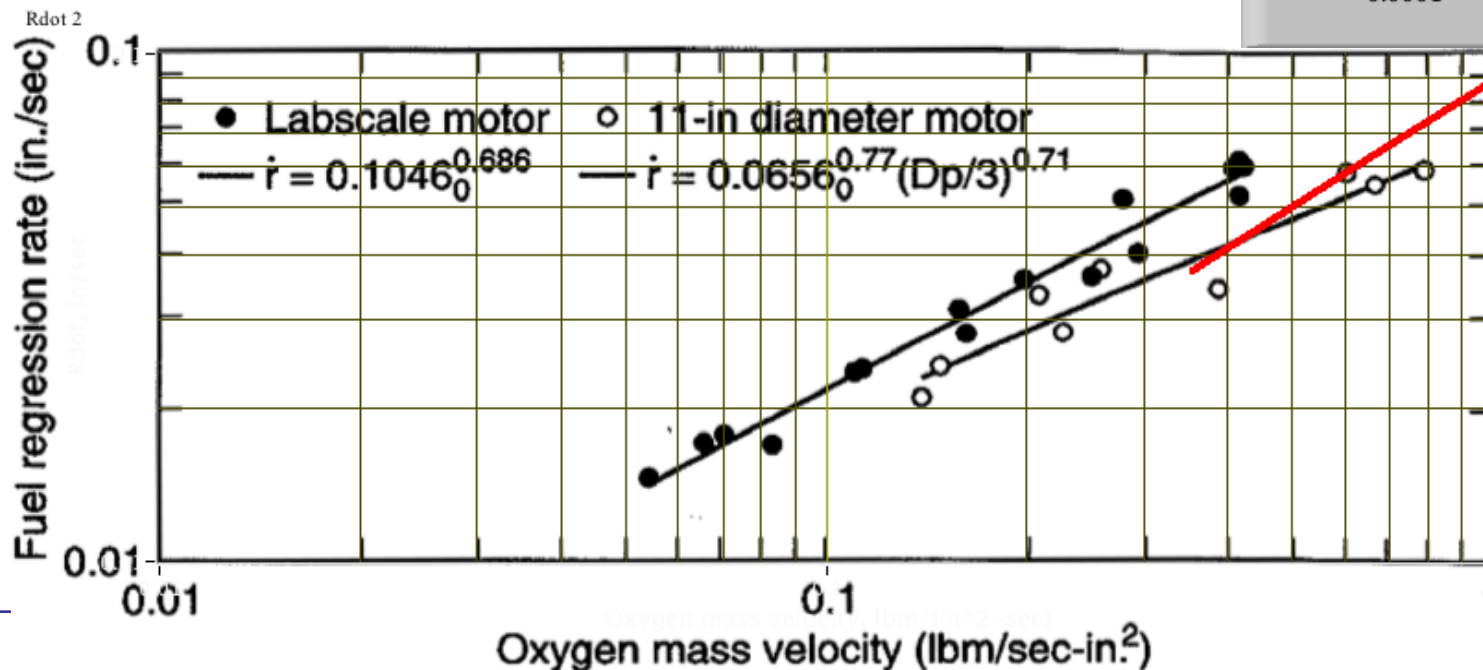
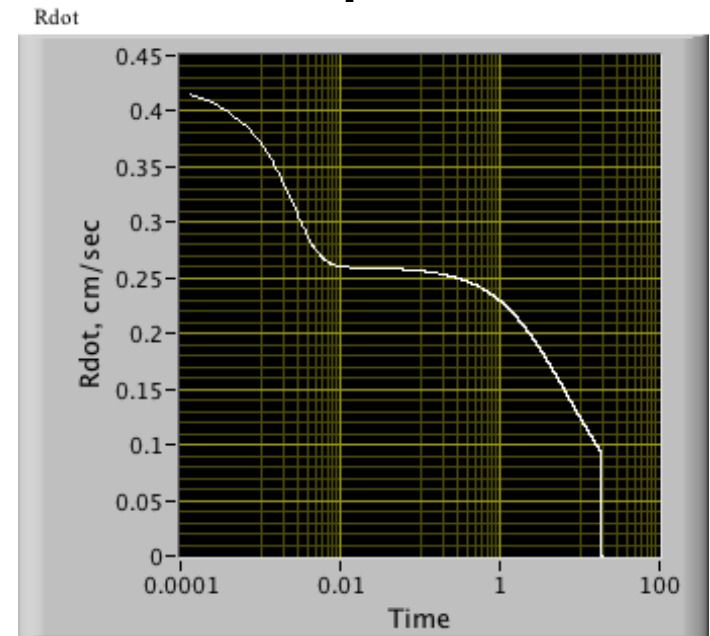


- Burn is Slightly Regressive

LOX/ HTPB Hybrid Numerical Example (cont'd)

- Compare Predictions to Data Plotted in Figure 15-8, Sutton and Biblarz (Page 591)

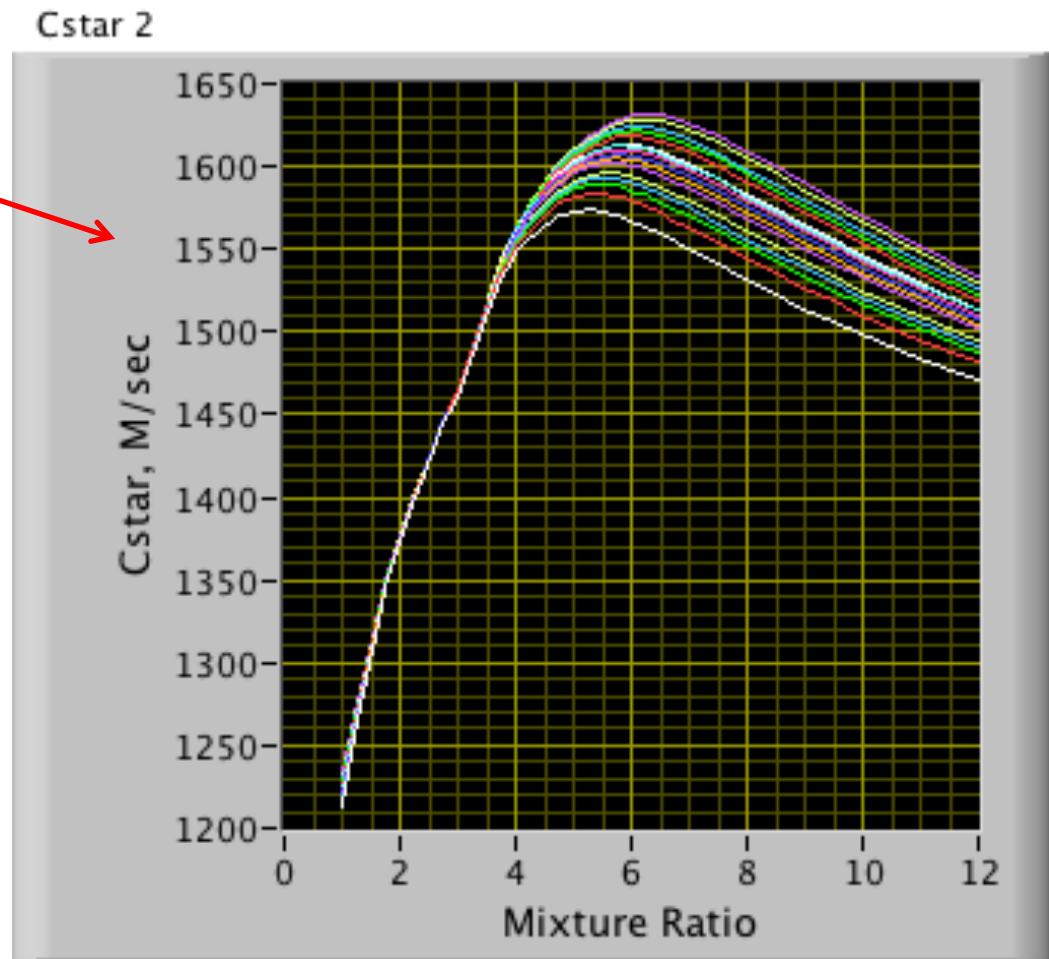
Burn coefficient ($n=4/5$) is slightly higher



Correcting for Total Port Massflux

- Original Model based on Oxidizer massflow... works well for propellants with naturally high required O/F ratio ... i.e. Nitrous Oxide and HTPB

.... But becomes less accurate for models with Lower O/F ratio design Points ... i.e. LOX/GOX Based systems where best O/F is < 2.0



Correcting for Total Port Massflux ⁽²⁾

- Rewrite regression rate equation in Generic form

$$\dot{r}_x = a \cdot G_{total}^n \cdot x^m$$

- Where $G(x)_{total} = G(x)_{ox} + \frac{\rho_{fuel}}{A_{port}} \cdot \int_0^x C_{port} \cdot \dot{r}(s) ds$

C_{port} = port circumference at station x

- Rewrite in terms of massflow

$$\dot{m}(x)_{total} = \dot{m}(x)_{ox} + \rho_{fuel} \cdot \int_0^x C_{port} \cdot \dot{r}(s) ds$$

Correcting for Total Port Massflux ⁽³⁾

- Convert to differential form

$$\frac{\partial \dot{m}(x)_{total}}{\partial x} = \rho_{fuel} \cdot C_{port} \cdot \dot{r}(x) \rightarrow \dot{m}(x)_{ox} \equiv constant$$

- Substitute for $\dot{r}(x)$

$$\frac{\partial \dot{m}(x)_{total}}{\partial x} = \rho_{fuel} \cdot C_{port} \cdot a \cdot G(x)^n \cdot x^m$$

- Rewrite massflow of massflux by dividing by port area

$$\frac{\partial G(x)_{total}}{\partial x} = \frac{\rho_{fuel} \cdot C_{port} \cdot a \cdot G(x)^n \cdot x^m}{A_{port}}$$

Correcting for Total Port Massflux ⁽⁴⁾

- Assume Cylindrical port and sub into previous equation

$$C_{port} = 2 \cdot \pi \cdot r(x)$$

$$A_{port} = \pi \cdot r(x)^2$$

$$\frac{\partial G(x)_{total}}{\partial x} = \frac{\rho_{fuel} \cdot 2 \cdot \pi \cdot r(x) \cdot a \cdot G(x)^n \cdot x^m}{\pi \cdot r(x)^2} =$$

$$\frac{2 \cdot \rho_{fuel} \cdot (a \cdot G(x)^n \cdot x^m)}{r(x)}$$

- Divide by mass flux

$$\frac{\partial G(x)_{total}}{G(x)^n} = \frac{2 \cdot a \cdot \rho_{fuel}}{r(x)} \cdot x^m \partial x$$

Correcting for Total Port Mass flux ⁽⁵⁾

- Replace local port radius by mean longitudinal average

$$\rightarrow r(x) \approx r_L = \frac{1}{L} \int_0^L r(s) \cdot ds$$

$$\frac{\partial G(x)_{total}}{\partial x} = \frac{2 \cdot \rho_{fuel} \cdot (a \cdot G(x)^n \cdot x^m)}{r_L}$$

- Separate Variables

$$\frac{\partial G(x)_{total}}{G(x)^n} = \left(\frac{2 \cdot a \cdot \rho_{fuel}}{r_L} \right) \cdot x^m \partial x$$

Correcting for Total Port Mass flux ⁽⁵⁾

- Integrate both sides to get solution

$$\frac{G(x)^{1-n}}{1-n} = \frac{2 \cdot a \cdot \rho_{fuel}}{r_L} \cdot \frac{x^{m+1}}{m+1} + C$$

- Apply Boundary Condition

$$= 0 \rightarrow G(x) = G_{ox} \rightarrow C = \frac{G_{ox}^{1-n}}{1-n}$$

$$\frac{G(x)^{1-n}}{1-n} = \frac{G_{ox}^{1-n}}{1-n} + \frac{2 \cdot a \cdot \rho_{fuel}}{r} \cdot \frac{x^{m+1}}{m+1} \rightarrow G(x)^{1-n} = G_{ox}^{1-n} + \left(\frac{1-n}{m+1} \right) \frac{2 \cdot a \cdot \rho_{fuel}}{r} \cdot x^{m+1}$$

Solve for Mean Longitudinal Port Massflux

$$\text{mean longitudinal mass flux} \rightarrow \bar{G}^{1-n} = \frac{1}{L} \int_0^L \left[G_{ox}^{1-n} + \left(\frac{1-n}{m+1} \right) \frac{2 \cdot a \cdot \rho_{fuel}}{\bar{r}} \cdot x^{m+1} \right] \cdot dx =$$

$$G_{ox}^{1-n} + \frac{1}{L} \left\{ \left(\frac{1-n}{m+1} \right) \frac{2 \cdot a \cdot \rho_{fuel}}{\bar{r}} \cdot \frac{x^{m+1} \cdot x}{m+2} \right\}_0^L = G_{ox}^{1-n} + \left(\frac{1-n}{m+1} \right) \frac{2 \cdot a \cdot \rho_{fuel}}{\bar{r}} \cdot \frac{L^{m+1}}{m+2}$$

$$\bar{G} = \left[G_{ox}^{1-n} + \left(\frac{1-n}{(m+1) \cdot (m+2)} \right) \frac{2 \cdot a \cdot \rho_{fuel}}{\bar{r}} \cdot L^{m+1} \right]^{\frac{1}{1-n}}$$

Correcting for Total Port Mass flux (6)

- Solve for Total Massflux

$$G(x) = \left(G_{ox}^{1-n} + \left(\frac{1-n}{m+1} \right) \frac{2 \cdot a \cdot \rho_{fuel}}{r_L} \cdot x^{m+1} \right)^{\frac{1}{1-n}}$$

- Solve for regression rate

$$\dot{r}_x = a \cdot \left(G_{ox}^{1-n} + \left(\frac{1-n}{m+1} \right) \frac{2 \cdot a \cdot \rho_{fuel}}{r_L} \cdot x^{m+1} \right)^{\frac{n}{1-n}} \cdot x^m$$

- Mean Longitudinal Regression rate

$$\bar{r} = a \cdot \bar{G}^n \cdot L^m = a \cdot \left[G_{ox}^{1-n} + \left(\frac{1-n}{(m+1) \cdot (m+2)} \right) \frac{2 \cdot a \cdot \rho_{fuel}}{\bar{r}} \cdot L^{m+1} \right]^{\frac{1}{1-n}} \cdot L^m$$

Correcting for Total Port Mass flux (7)

- Check Expression

$$\bar{r} = a \cdot \left(G_{ox}^{1-n} + \left(\frac{1-n}{(m+1) \cdot (m+2)} \right) \frac{2 \cdot a \cdot \rho_{fuel} \cdot L^{m+1}}{r_L} \right)^{\frac{n}{1-n}} \cdot L^m$$

Dimensional Analysis: $\frac{2 \cdot a \cdot \rho_{fuel} \cdot L^{m+1}}{r(x)} \rightarrow a \sim \frac{M}{s} \cdot \left(\frac{s - M^2}{kg} \right)^n \cdot \frac{1}{M^m}$

$$\frac{M}{s} \cdot \left(\frac{s - M^2}{kg} \right)^n \cdot \frac{1}{M^m} \cdot \frac{kg}{M^3} \cdot \frac{1}{M} \cdot M^{m+1} =$$

$$\left(\frac{s - M^2}{kg} \right)^n \cdot \frac{1}{M^m} \cdot \frac{1}{M} \cdot \frac{kg}{s - M^2} \cdot M^{m+1} = \frac{1}{M^m} \cdot \left(\frac{kg}{s - M^2} \right)^{1-n} \cdot M^m = \left(\frac{kg}{s - M^2} \right)^{1-n}$$

$$G_{ox}^{1-n} \sim \left(\frac{kg}{s - M^2} \right)^{1-n}$$

Check!

Correcting for Total Port Mass flux (8)

- Use Classical values for $\{n, m\} = \{4/5, -1/5\}$

$$\left. \begin{array}{l} n = 4/5 \\ m = -1/5 \end{array} \right\} \rightarrow \bar{r} = a \cdot \frac{\left(G_{ox}^{1/5} + \frac{1/5}{4 \cdot 9} \frac{2 \cdot a \cdot \rho_{fuel} \cdot L^{4/5}}{r} \right)^{4/5}}{L^{1/5}} = a \cdot \frac{\left(G_{ox}^{1/5} + \frac{5 a \cdot \rho_{fuel} \cdot L^{4/5}}{9 \cdot 2 \cdot r} \right)^4}{L^{1/5}} = a \cdot \frac{\left(G_{ox}^{1/5} + \frac{5 a \cdot \rho_{fuel} \cdot L^{4/5}}{9 D_{port}} \right)^4}{L^{1/5}}$$

$$a = \left(\frac{0.047}{P_r^{2/3} \cdot \rho_{fuel}} \right) \cdot \left(\frac{\Delta h_{flame\ surface}}{h_v} \right)^{0.23} \cdot \mu^{1/5} \rightarrow \bar{r} = \left(\frac{0.047}{P_r^{2/3} \cdot \rho_{fuel}} \right) \cdot \left(\frac{\Delta h_{flame\ surface}}{h_v} \right)^{0.23} \cdot \left(G_{ox}^{1/5} + \frac{5 a \cdot \rho_{fuel} \cdot L^{4/5}}{9 D_{port}} \right)^4 \cdot \left(\frac{\mu}{L} \right)^{1/5}$$

$$\bar{r} = \left(\frac{0.047}{P_r^{2/3} \cdot \rho_{fuel}} \right) \cdot \left(\frac{\Delta h_{flame\ surface}}{h_v} \right)^{0.23} \cdot \left(G_{ox}^{1/5} + \frac{5}{9} \cdot \left(\frac{0.047}{P_r^{2/3}} \right) \cdot \left(\frac{\Delta h_{flame\ surface}}{h_v} \right)^{0.23} \cdot \left(\frac{\mu}{L} \right)^{1/5} \cdot \left(\frac{L}{D_{port}} \right) \right)^4 \cdot \left(\frac{\mu}{L} \right)^{1/5}$$

Correcting for Total Port Mass flux (8)

- Compare to Oxidizer-flux Only Model
- Total Mass flux

$$\bar{\dot{r}} = \left(\frac{0.047}{P_r^{2/3} \cdot \rho_{fuel}} \right) \cdot \left(\frac{\Delta h_{flame\ surface}}{h_v} \right)^{0.23} \cdot \left(G_{ox}^{1/5} + \frac{5}{9} \cdot \left(\frac{0.047}{P_r^{2/3}} \right) \cdot \left(\frac{\Delta h_{flame\ surface}}{h_v} \right)^{0.23} \cdot \left(\frac{\mu}{L} \right)^{1/5} \cdot \left(\frac{L}{D_{port}} \right)^4 \right) \cdot \left(\frac{\mu}{L} \right)^{1/5}$$

- Oxidizer-Only Mass Flux

$$\bar{\dot{r}} = \left(\frac{0.047}{P_r^{2/3} \cdot \rho_{fuel}} \right) \cdot \left(\frac{\Delta h_{flame\ surface}}{h_v} \right)^{0.23} \cdot G_{ox}^{4/5} \cdot \left(\frac{\mu}{L} \right)^{1/5}$$

Revisit O/F Shift with Total Flux Model

- Compare to Oxidizer-flux Only Model

$$O/F = \frac{\dot{m}_{ox}}{\dot{m}_{fuel}} = \frac{\dot{m}_{ox}}{\rho_{fuel} \cdot 2 \cdot \pi \cdot r_L \cdot \dot{r}_L \cdot L} = \frac{\dot{m}_{ox}}{\rho_{fuel} \cdot 2 \cdot \pi \cdot r_L \cdot L \cdot a \cdot \left(G_{ox}^{1-n} + \left(\frac{1-n}{(m+1)(m+2)} \right) \frac{2 \cdot a \cdot \rho_{fuel} \cdot L^{m+1}}{r_L} \right)^{\frac{n}{1-n}} \cdot L^m}$$

Multiply numerator and denominator by $(\pi \cdot r_L^2)^n$

$$O/F = \frac{\dot{m}_{ox} \cdot (\pi \cdot r_L^2)^n}{\rho_{fuel} \cdot 2 \cdot \pi \cdot r_L \cdot a \cdot \left[G_{ox}^{1-n} + \left(\frac{1-n}{(m+1)(m+2)} \right) \frac{2 \cdot a \cdot \rho_{fuel} \cdot L^{m+1}}{r_L} \right] \cdot (\pi \cdot r_L^2)^{\frac{n}{1-n}} \cdot L^{1+m}} =$$

$$\frac{\dot{m}_{ox} \cdot (\pi \cdot r_L^2)^n}{\rho_{fuel} \cdot 2 \cdot \pi \cdot r_L \cdot a \cdot \left(\dot{m}_{ox}^{1-n} + \left(\frac{1-n}{(m+1)(m+2)} \right) \frac{2 \cdot a \cdot \rho_{fuel} \cdot L^{m+1}}{r_L} \cdot (\pi \cdot r_L^2)^{1-n} \right)^{\frac{n}{1-n}} \cdot L^{1+m}} =$$

$$\frac{\dot{m}_{ox} \cdot \pi^{n-1} \cdot r_L^{2n-1}}{\rho_{fuel} \cdot 2 \cdot a \cdot \left(\dot{m}_{ox}^{1-n} + \left(\frac{1-n}{(m+1)(m+2)} \right) \pi^{1-n} \cdot 2 \cdot a \cdot \rho_{fuel} \cdot L^{m+1} \cdot r_L^{1-2n} \right)^{\frac{n}{1-n}} \cdot L^{1+m}}$$

Instantaneous mixture (O/F) ratio (4)

for near-cylindrical port \rightarrow

$$\begin{aligned} A_{burn} &= \pi \cdot D \cdot L \\ A_{c\ chamber} &= \frac{\pi}{4} D^2 \end{aligned}$$

In terms of generic model based on $G_{ox} \dots$ $\dot{r}_x = a \cdot G_{ox}^n \cdot x^m$

$$\begin{aligned} O/F &= \frac{\dot{m}_{ox}}{\dot{m}_{fuel}} = \frac{\dot{m}_{ox}}{\rho_{fuel} \cdot (2 \cdot \pi \cdot r_L \cdot L) \cdot \dot{r}_L} = \frac{\dot{m}_{ox}}{\rho_{fuel} \cdot (2 \cdot \pi \cdot r_L \cdot L) \cdot a \cdot G_{ox}^n \cdot L^m} = \\ &= \frac{\dot{m}_{ox}}{\rho_{fuel} \cdot (2 \cdot \pi \cdot r_L \cdot L) \cdot a \cdot \left(\frac{\dot{m}_{ox}}{\pi \cdot r_L^2} \right)^n \cdot L^m} = \frac{\dot{m}_{ox}^{1-n} \cdot r_L^{2n-1}}{\rho_{fuel} \cdot 2 \cdot a \cdot L^{1-m}} \end{aligned}$$

$$r_L = \frac{D_{port}}{2} \rightarrow \boxed{O/F = \frac{\dot{m}_{ox}^{1-n} \cdot r_L D_{port}^{2n-1}}{\rho_{fuel} \cdot 2 \cdot 2^{2n-1} a \cdot L^{1-m}} = \frac{\dot{m}_{ox}^{1-n} \cdot r_L D_{port}^{2n-1}}{\rho_{fuel} \cdot 4^n a \cdot L^{1-m}}}$$

$n = 1/2 \rightarrow$ No O/F shift !

Revisit O/F Shift with Total Flux Model (2)

- Let $\{n, m\} = \{1/2, -1/2\}$ based on total flux

$$O/F = \frac{\dot{m}_{ox} \cdot \pi^{\frac{1}{2}-1} \cdot r_L^{2\frac{1}{2}-1}}{\rho_{fuel} \cdot 2 \cdot a \cdot \left(\dot{m}_{ox}^{1-\frac{1}{2}} + \left(\frac{1-\frac{1}{2}}{\left(-\frac{1}{2}+1\right)\left(-\frac{1}{2}+2\right)} \right) \pi^{1-\frac{1}{2}} \cdot 2 \cdot a \cdot \rho_{fuel} \cdot L^{-\frac{1}{2}+1} \cdot r_L^{1-2\frac{1}{2}} \right)^{\frac{\frac{1}{2}}{1-\frac{1}{2}}} \cdot L^{1-\frac{1}{2}}} =$$

$$\frac{\dot{m}_{ox}}{\rho_{fuel} \cdot 2 \cdot a \cdot \sqrt{\pi} \left(\dot{m}_{ox}^{\frac{1}{2}} + \sqrt{\pi} \cdot \frac{4}{3} \cdot a \cdot \rho_{fuel} \cdot L^{\frac{1}{2}} \right) \cdot L^{\frac{1}{2}}} \rightarrow \text{no...O/F shift!}$$

Questions??

